5-25-1954

An Experimental and Theoretical Investigation of the Characteristics of a Magnetic Amplifier

Merle H. Wittmeyer

Recommended Citation

Wittmeyer, Merle H.. "An Experimental and Theoretical Investigation of the Characteristics of a Magnetic Amplifier." (1954). https://digitalrepository.unm.edu/ece_etds/413

Wittmeyer — Characteristics of a Magnetic Amplifier

UNIVERSITY OF NEW MEXICO LIBRARY

MANUSCRIPT THESES

This thesis by Merle H. Wittmeyer has been used by the following persons, whose signatures attest their acceptance of the above restrictions.

NAME AND ADDRESS	DATE

AN EXPERIMENTAL AND THEORETICAL INVESTIGATION OF THE CHARACTERISTICS OF A MAGNETIC AMPLIFIER

By

Merle H. Wittmeyer

A Thesis
In partial fulfillment of the
Requirements for the Degree of
Master of Science in Electrical Engineering

The University of New Mexico
1954

This thesis, directed and approved by the candidate's committee, has been accepted by the Graduate Committee of the University of New Mexico in partial fulfillment of the requirements for the degree of

MASTER OF SCIENCE

E F Castetter
DEAN

DATE 5/25/54

Thesis committee

Ralph W. Tapy
CHAIRMAN

Robert A. Herseme Jr.

J. L. Ellis

This thesis, directed and approved [illegible] mittee, has been accepted by the Graduate [illegible] University of New Mexico in partial fulfillment of the requirements for the degree of

MASTER OF [illegible]

Dean

3/25/

Date

Thesis committee

TABLE OF CONTENTS

APPENDIX PAGE

LIST OF TABLES

TABLE PAGE

LIST OF FIGURES

CHAPTER I

THE PROBLEM AND METHOD OF INVESTIGATION

Many excellent analyses of magnetic amplifiers have been published. As in every investigation, however, there are many details not explained. The purpose of this investigation was to explain some of the details of magnetic amplifier characteristics.

I. THE PROBLEM

Specifically, the static characteristics of a magnetic amplifier were determined experimentally and analyzed in more detail than had previously been done.

Most magnetic amplifier analyses present and analyze the transfer characteristics. There is, however, much to be said in favor of the characteristic curve method. The latter method was used in this investigation.

In addition, most analyses have been limited to the regions near the point of maximum power gain, an important region and one that can be easily analyzed.

However, the characteristics in the region of larger load resistance are also interesting and may, in some cases, be more useful than those in the region usually studied.

This investigation extended both the experimental and theoretical study into the large load region.

II. METHOD OF INVESTIGATION

The experimental work consisted of the necessary studies for instrumentation and the actual determination of the amplifier static characteristics.

The theoretical study consisted of calculation of the usual first approximation to the characteristics, analysis of the errors of this method, and computation of the necessary corrections to extend the region of analysis.

CHAPTER II

EXPERIMENTAL INVESTIGATION OF THE STATIC CHARACTERISTICS OF A MAGNETIC AMPLIFIER

In general, a magnetic amplifier is used to control the voltage, current or power of some load. If it is to be an amplifier, then the variation in output voltage, current or power must be greater respectively than the variation in control voltage, current or power.

The output of a magnetic amplifier is a function of both the control signal and of the size and character of the load. Its characteristics may then be portrayed as a family of curves of either constant control signal or constant load. The former method was used in this investigation and is described in Section I. of this chapter. The details of experimental technique are included in Section II. The actual results of the experiment and the conclusions are contained in Section III.

I. THE EXPERIMENTAL METHOD

The magnetic amplifier used in this project was a Vickers number 36A34 educational magnetic amplifier used with the DD1 connections. A diagram of the amplifier with associated load is shown in Figure 1. In the diagram R_L is the load resistance, and N_g and N_c are respectively the

PART II

EXPERIMENTAL DETERMINATION OF THE STATIC CHARACTERISTICS OF A MAGNETIC AMPLIFIER

In general, a magnetic amplifier is used to control the voltage, current or power of some load. If it is to be an amplifier, then the variation in output voltage, current or power must be greater respectively than the variation in control voltage, current or power.

The output of a magnetic amplifier is a function of both the control signal and of the size and character of the load. Its characteristics can be portrayed as a family of curves of either constant control signal or constant load. The former method was used in this investigation and is described in Section I of this part. The details of the experimental technique are discussed in Section II. The final results of the experiment and the conclusions are contained in Section III.

I. THE EXPERIMENTAL METHOD

The magnetic amplifier used in this investigation is a Vickers number [illegible] [illegible] magnetic amplifier rated with the DC arrangement. A diagram of the amplifier and its associated load is shown in Figure 1. In the diagram, R is the load resistance, R_c and R_s are respectively the

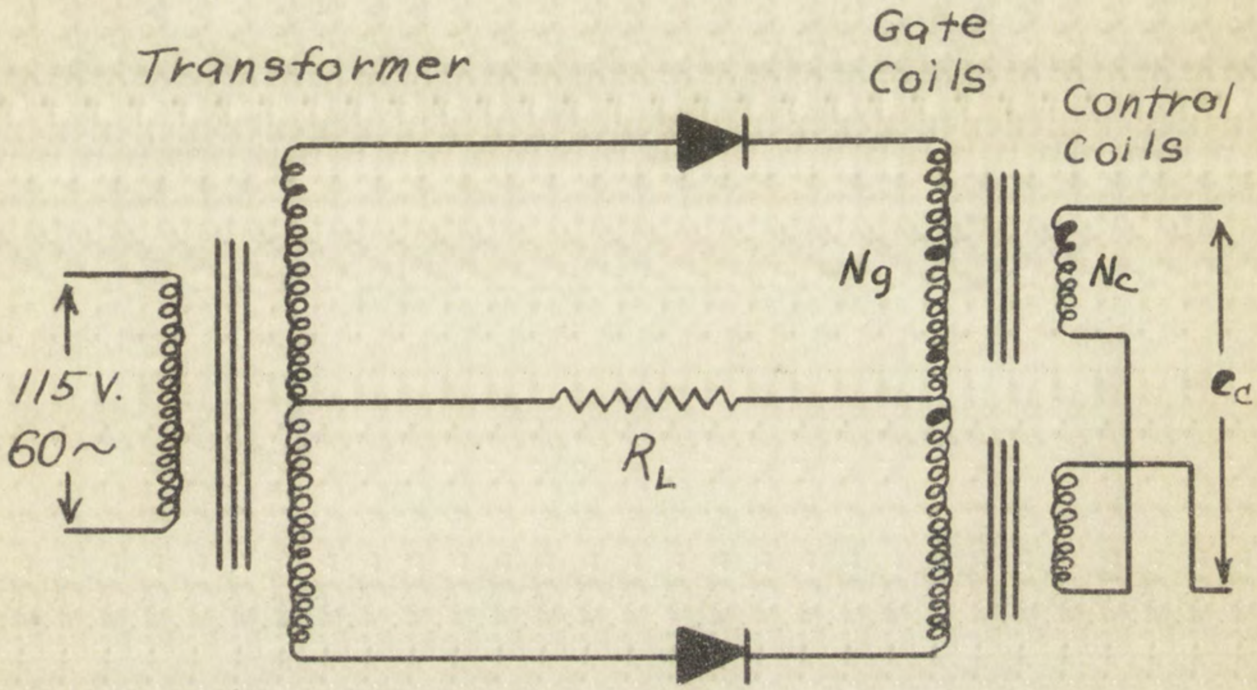

Figure 1

Experimental Connection Diagram

for Vickers Type 36A34 DD1

Educational Magnetic Amplifier

turns of the gate and control windings of the two reactors.

Leaving the details of analysis to Chapter III, it may be stated briefly that such a magnetic amplifier is a controlled, full-wave, center-tapped rectifier. Control is obtained by increasing the current through the control windings, which results in the reactors saturating sooner in each cycle and thus increasing the output.

In this experiment the simple case of a purely resistive load was used. Arbitrarily, the voltage amplification was analyzed, rather than power or current.

As mentioned previously, the magnetic amplifier characteristics can be presented as a family of curves of constant load resistance. Such a set of curves is shown in Figure 2. Such curves may be obtained by holding all perameters constant except the control signal, which is varied smoothly over the control range. A record is made of the load resistance used and of corresponding values of input and output. The load resistance is next changed to some other value and the process repeated until the family of curves has been obtained.

If, in a specific application, the load resistance coincides with the value for one of the curves, then the amplifier output can readily be determined. On the other hand, if some intermediate value of load resistance is used, then the output can be found only by interpolation

turns of the external [illegible] windings of the two reactors.

[illegible] the [illegible] of analysis to Figure [illegible], it may be stated [illegible] that in the magnetic amplifier, as a controlled, half-wave, [illegible] amplifier, control is obtained by [illegible] the [illegible] and [illegible] the control windings, [illegible] saturation in each cycle [illegible].

In this [illegible] a [illegible] sistive load [illegible], the magnetic amplification was [illegible] power [illegible].

An [illegible] the magnetic amplifier characteristics [illegible] as a family of curves of constant load resistance. [illegible] a set of curves is shown in Figure 2. [illegible] curves may be [illegible] all parameters constant except [illegible] varied [illegible] over the [illegible] range. [illegible] of the load resistance [illegible] corresponding values of input and output [illegible] be some other value [illegible] the family of curves has been [illegible].

If, [illegible], the load resistance coincides with the value for one of the curves, then the amplifier output [illegible]. On the other hand, if [illegible] load resistance is used, then the [illegible]

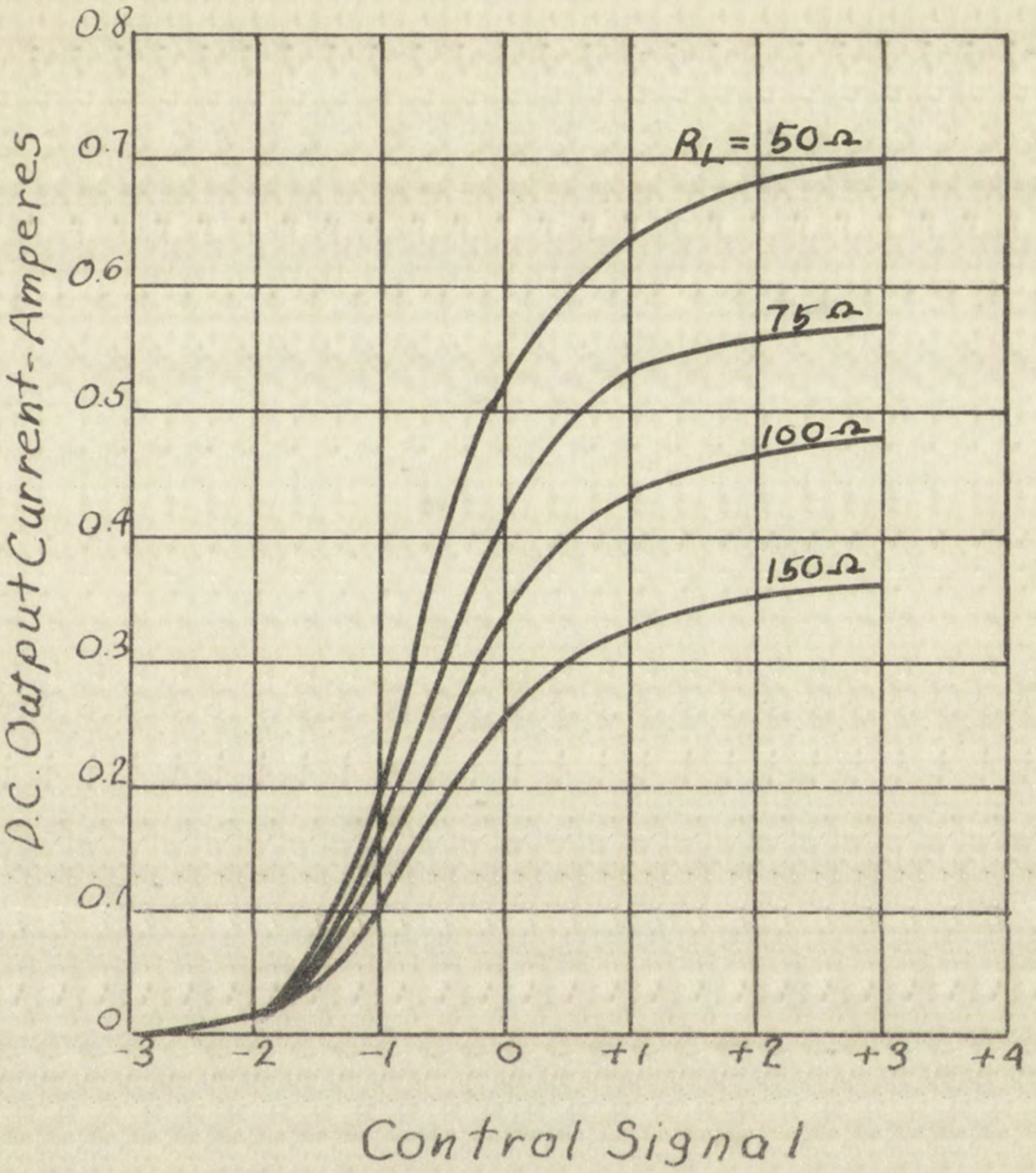

Figure 2

Typical Transfer Curves

For A Magnetic Amplifier

between the irregularly curved lines. This is neither an easy nor an accurate process.

Due to its greater flexibility and as an aid to analysis, a method was used in the experimental investigation which is practically the same as, and was suggested by, the method of obtaining direct-current generator external characteristics. Literature obtained later showed that this was not an original application.[1]

The magnetic amplifier was connected as shown in Figure 3. The autotransformer was used to adjust the supply voltage, E_{ac}, read by voltmeter, V_1, so that the applied voltage was always 115 rms. volts either side of the center tap. To obtain the characteristic curves of the amplifier, the control voltage, e_c, read on voltmeter, V_3, was set to the desired value by adjusting the direct-current supply source, E_c, and the resistor, R_2.

The load resistance, R_L, was then varied over the required range and corresponding readings taken of the direct-current load voltage, E_L, on voltmeter, V_2, and the load direct current, I_L, on ammeter, A_1. Other control voltages were then selected and the process repeated until the desired data had been obtained. These data are recorded in Table 1 and plotted in Figure 4.

---

[1] Bulletin 20-B on Magnetic Amplifiers, (Vickers Electric Division. St. Louis, 1950).

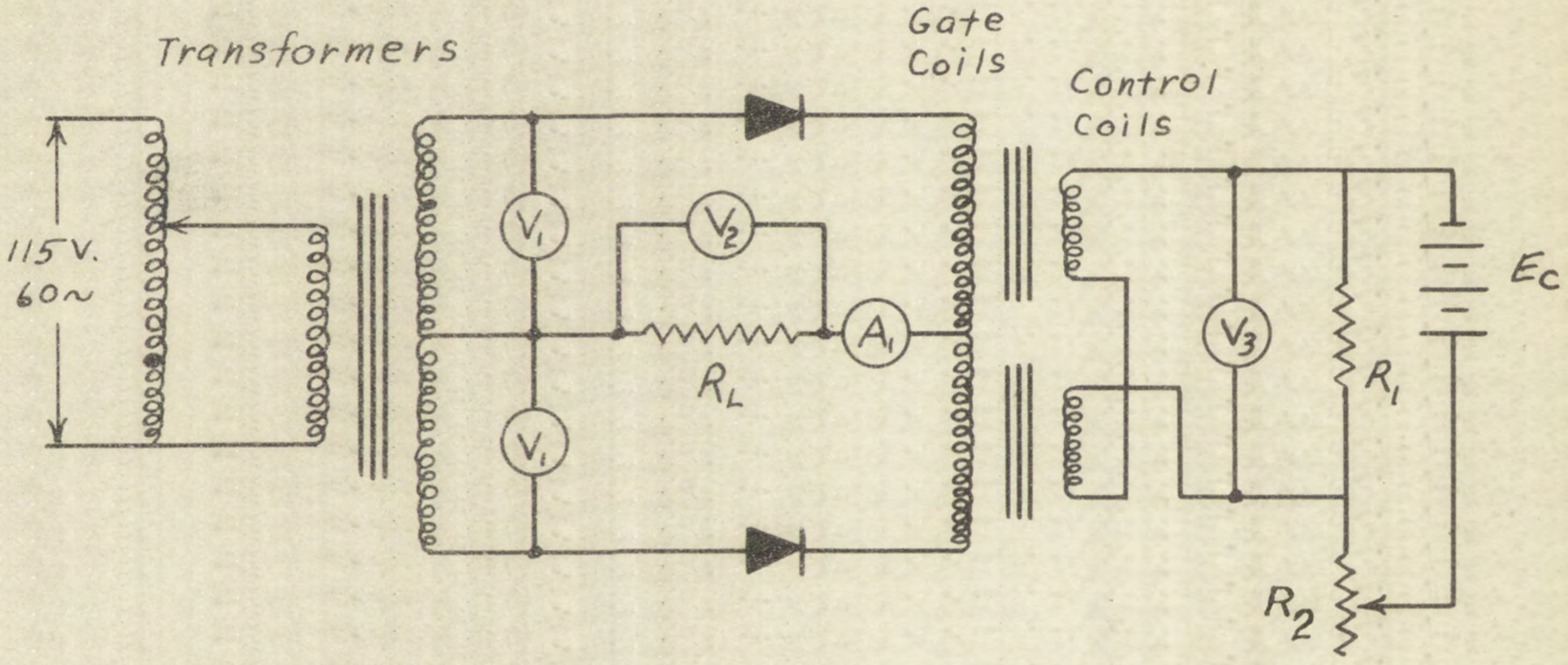

Figure 3

Magnetic Amplifier in Circuit for

Measuring Characteristics

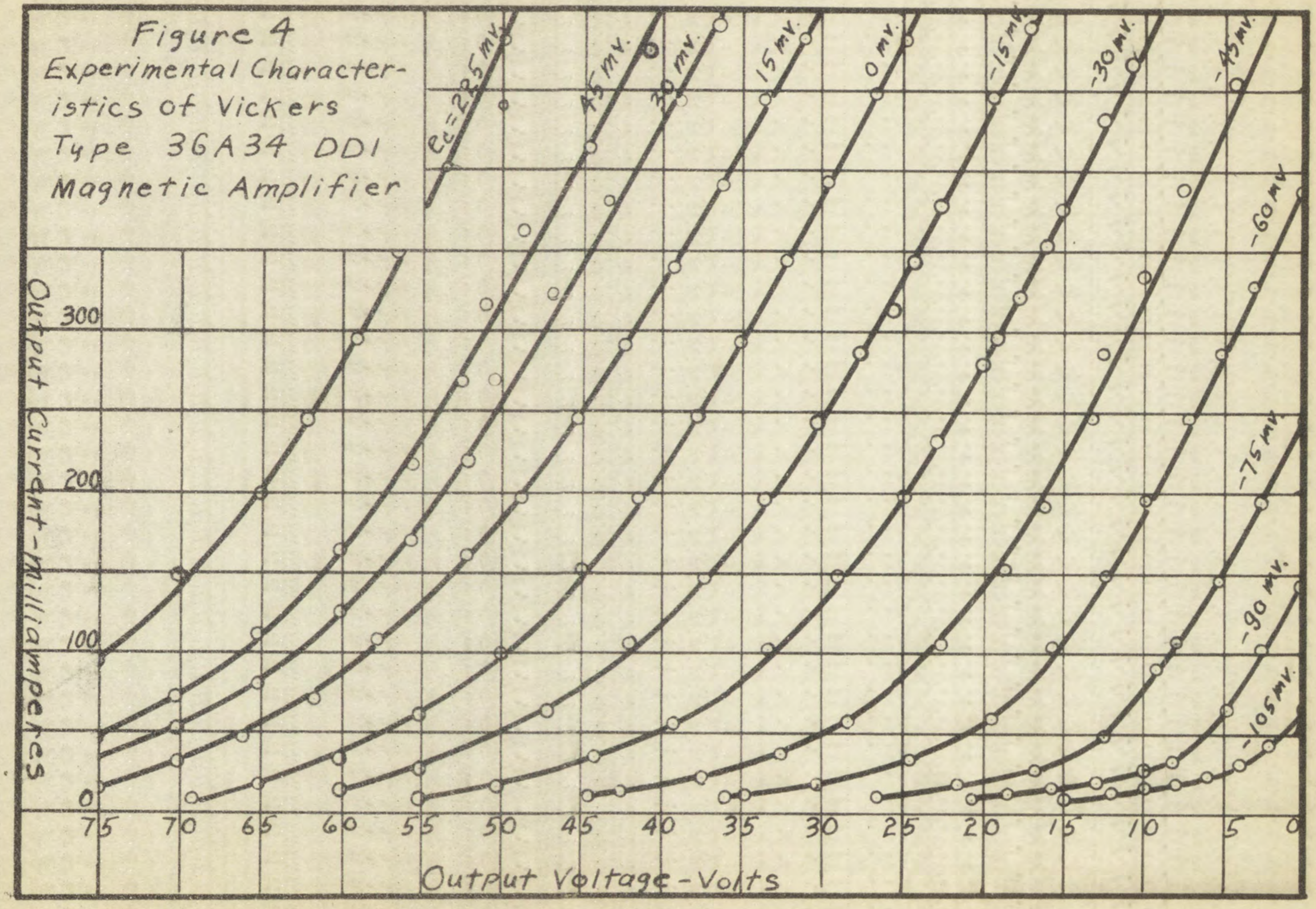

Figure 4
Experimental Characteristics of Vickers
Type 36A34 DDI
Magnetic Amplifier

II. EXPERIMENTAL DETAILS AND TECHNIQUE

To minimize the chance of drawing erroneous conclusions, all meters were calibrated. Standard calibration procedures were used.[2] Since a reliable standard cell was not available, the 1.0 volt position of the 1.5 volt direct-current scale of a Simpson Model 260 multimeter was arbitrarily selected as a standard after comparison with a one-quarter per cent dynamometer voltmeter. By the use of potentiometric methods all other voltmeters and ammeters were calibrated relative to this assumed standard. The dynamometer type voltmeter was used to transfer calibration to the alternating-current meters. All resistances used in the potentiometer had guaranteed accuracies within one per cent. Reading errors on all instruments were within one per cent. Actual errors in meter data should be within two per cent.

To aid in the theoretical analysis, additional data were obtained. The resistance of all windings and the inductance of each gate winding of the amplifier were measured with a General Radio Type 650A impedance bridge. For the values measured, the rated accuracy of this bridge is one per cent for resistance and ten per cent for inductance.

---

[2] Smith, Arthur Whitmore, Electrical Measurements in Theory and Application (New York: McGraw-Hill Book Company, Inc., 4th Ed., 1948).

[illegible]

To minimize the chance of [illegible] conditions, all meters were [illegible] calibration procedures were used.[8] Since a reliable [illegible] was not available, the 1.0 volt position of the 1.5 volt direct-current scale of a [illegible] 430 multimeter was arbitrarily selected as a standard after comparison with a one-quarter per cent [illegible] volt meter. By the use of potentiometric methods all other voltmeters and ammeters were calibrated relative to this standard meter. The dynamometer type voltmeter was used to transfer calibration to the alternating-current meters. The [illegible] used in the [illegible] and [illegible] accurate within one per cent; readings [illegible] all instruments were within one per cent. [illegible] errors in meter [illegible] within two per cent.

To aid in the theoretical analysis, additional data were obtained. The resistance of all windings and inductance of each [illegible] of the [illegible] were measured with a General Radio [illegible] bridge [illegible] the values measured. The [illegible] be [illegible] one per cent for [illegible] and [illegible] per cent for inductance.

---

[8] [illegible], *Electrical Measurements in Theory and Application* [illegible] (New York: McGraw-Hill Book Company, Inc., [illegible]).

Oscillograms were made which showed the variation of output wave-shape, both for variation in load resistance and variation in control signal. An electronic switch was used with the oscilloscope to superimpose the sixty cycle power source wave-shape.

The voltage-current characteristics of one of the rectifiers were measured. These data are recorded in Table II of Appendix C and graphed in Figure 15 of Appendix B.

III. RESULTS, CONCLUSIONS AND COMPARISONS

With the external characteristics of the magnetic amplifier plotted as in Figure 4 it is very easy to determine the output to any desired resistive load. If some load voltage is assumed, the corresponding load current may be calculated by ohms law. The load line for this resistance is then drawn from the origin through the point determined by the corresponding values of load current and voltage. Several such load lines have been drawn on the characteristic curves in Figure 5.

The output voltage corresponding to a given control voltage can, of course, be read on the voltage scale directly below the intersection of the load line and the curve for the control voltage.

For loads in the vicinity of 100 to 200 ohms there

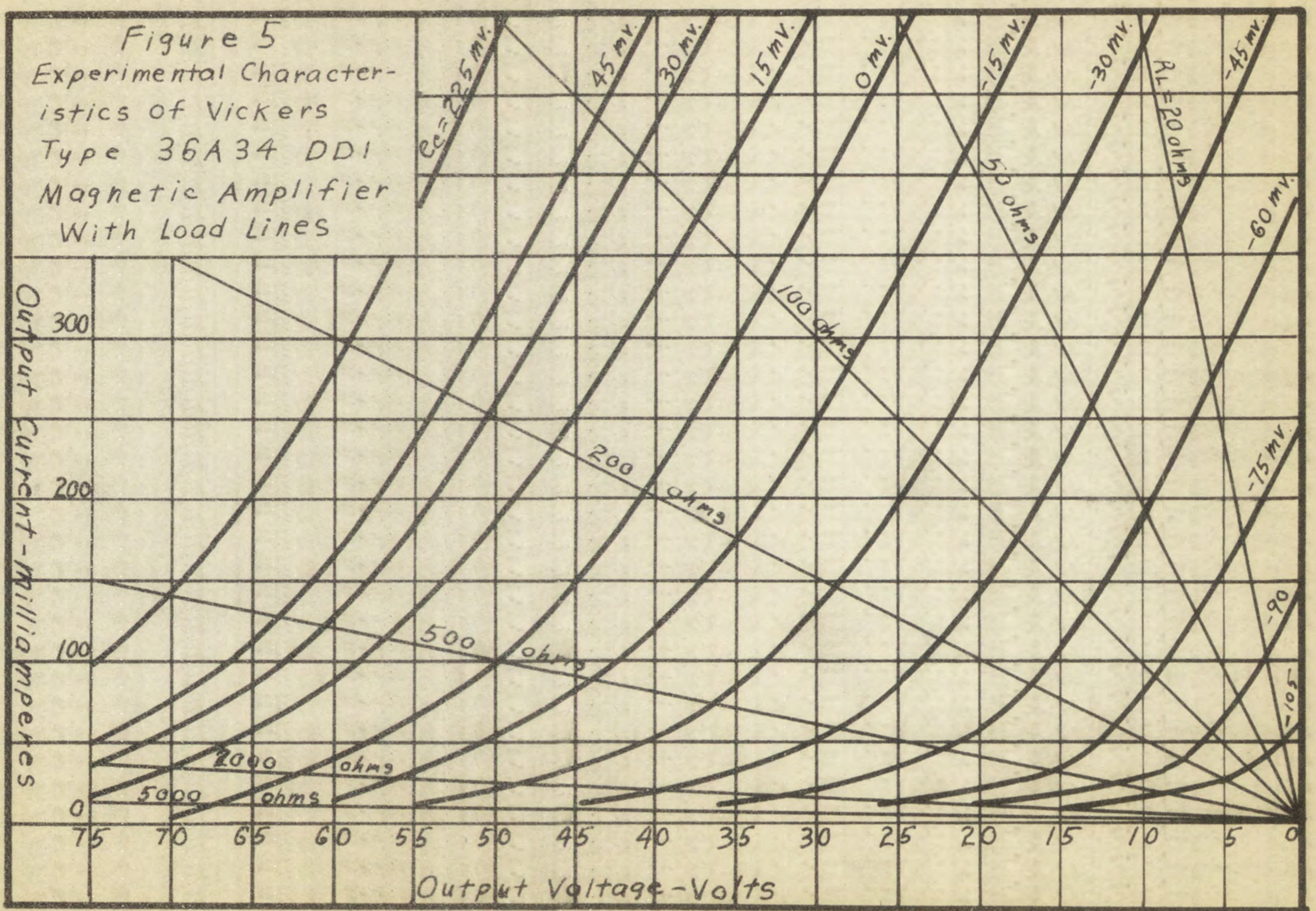

Figure 5
Experimental Characteristics of Vickers Type 36A34 DD1 Magnetic Amplifier With Load Lines

is a center region which gives quite linear amplification, while at either extreme of control current the amplification decreases. Loads of lower resistance than 100 ohms may cause excessively large load current to flow. Loads of 200 ohms or more produce load lines which lie in the curved region of the control curves. However, control is still reasonably linear over nearly as large a region as with a 100 ohm load until the load resistance becomes larger than 500 ohms.

There is a striking similarity between the characteristics of the magnetic amplifier in Figure 4 and the characteristics of a triode vacuum tube. The only major difference is that there is no voltage scale for the total applied voltage, only a scale for the voltage across the load.

It is at once obvious that the method of linear approximations[3] can be applied to the amplifier characteristics in the linear region to obtain an equivalent circuit for low frequency operation, using a resistance, R_g, corresponding to the plate resistance of a vacuum tube, and an amplification factor, μ , exactly the same as the μ of a vacuum tube. Computations, shown in Appendix A,

---

[3] Martin, Thomas L. Jr., Electronic Circuits (New York: Prentice-Hall, Inc., to be published 1954).

is a center region which gives quite linear amplification, while at either extreme of control current the amplification decreases. Loads of lower resistance than 100 ohms may cause excessively large load current to flow. Loads of 200 ohms or more produce load lines which lie on the curved region of the control curves. However, output is still reasonably linear over nearly the entire region, as with a 100 ohm load until the load resistance becomes larger than 500 ohms.

There is a striking similarity between the characteristics of the magnetic amplifier in Figure 4 and the characteristics of a triode vacuum tube. The only major difference is that there is no [illegible] for the total applied voltage, only a [illegible] for the [illegible] load.

It is [illegible] evident that the methods of linear approximation can be applied to the magnetic amplifier characteristics in the linear region to obtain an equivalent circuit for the small signal operation, using a resistance, r_p, corresponding to the plate resistance of a vacuum tube, and an amplification factor, μ, exactly the same as the μ of a vacuum tube. [illegible], shown in Appendix A.

---

[5] Martin, Thomas L. Jr., Electronic Circuits, New York: Prentice-Hall, Inc., to be published 1955.

yield average values of $R_g = 58$ ohms and $\mu = 500$. The equivalent circuit[4] of the amplifier is shown in Figure 6. From this the voltage amplification is given by

$$A = \frac{e_L}{e_c} = \mu \frac{R_L}{R_g + R_L} . \qquad (1)$$

---

[4] Ibid.

CHAPTER III

THEORETICAL INVESTIGATION OF THE MAGNETIC AMPLIFIER

In this chapter, an approximate analysis of the magnetic amplifier is presented in Section I. In Section II some of the errors of the approximate method are indicated and the necessary corrections computed. In Section III the final theoretical and the experimental results are compared.

I. THE APPROXIMATE ANALYSIS

As stated previously, the type of magnetic amplifier studied is essentially a controlled rectifier. Since such rectifiers have been thoroughly analyzed elsewhere[5], the remaining problems are concerned with the properties of the controlling elements.

In a magnetic amplifier these control elements consist of coils, often called gate windings, placed in each rectifier leg. These coils have ferromagnetic cores which are characterized by hysteresis loops with small area and nearly rectangular shape, closely approximating the idealized hysteresis loop shown in Figure 7. Control windings

---

[5] Davis, W. L. and Weed, H. R., Industrial Electronic Engineering (New York: Prentice-Hall, Inc., 1953) Chapters 3 and 4.

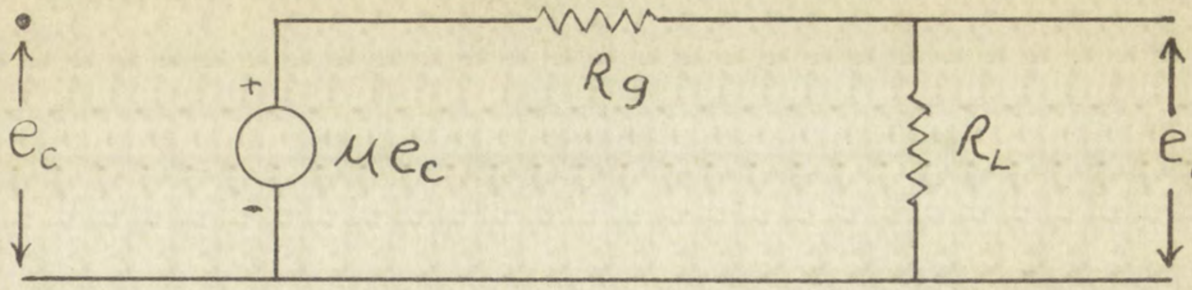

Figure 6

Equivalent Circuit of Vickers Type

36A34 DDI Magnetic Amplifier

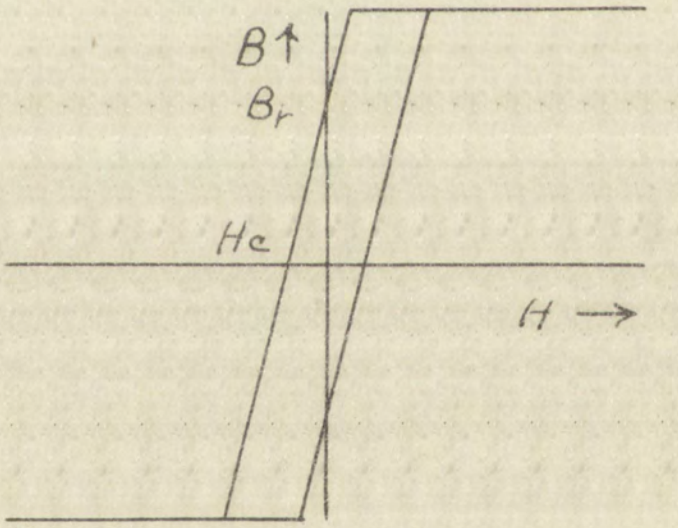

Figure 7

Idealized Hysteresis Loop

are placed on each core.

Under steady state conditions, at the beginning of alternate half cycles, the associated rectifier allows voltage to be applied across its gate winding in series with the load. At this time there will be some initial value of magnetic flux in the core, due to both the control signal and the reset[6] signal received during the non-operating half cycle. If the sum of the load and gate resistances is much less than the reactance of the unsaturated core, then essentially all the applied voltage will appear across the gate winding inductance, necessitating a change in flux which at any time will be given by

$$\Delta\phi = \frac{1}{N_g}\int_0^t e\,dt = \frac{1}{N_g}\int_0^t E_m \sin \omega t \, dt \qquad (2)$$

if the applied voltage is sinusoidal. When the core flux reaches the saturation value the inductance of the core becomes zero, assuming a flat top on the hysteresis loop, and all applied voltage appears across the gate and load resistances. With the assumptions made, the load current suddenly increases at saturation to many times the value before saturation. The load, or gate, current for such a half cycle of operation is shown in Figure 8. For a full-wave type rectifier this wave-shape is repeated each half

---

[6] Ramey, R. A., <u>On The Control of Magnetic Amplifiers</u> AIEE Trans., Vol. 70, Part II, pp. 2124-2128.

are placed on each core.

Under steady state conditions, at the beginning of alternate half cycles, the saturable reactor permits all the voltage to be applied across the gate windings in series with the load. At this time the core will be at some initial value of magnetic flux in the core, due to both the control signal and the reset signal received during the non-operating half-cycle. If the sum of the rectifier and gate resistances in each lead from the terminals of the unsaturated core, then essentially all the applied voltage will appear across the gate windings. Consequently, a change in flux level at any time will be given by

$$\Delta\phi = \frac{1}{N_g}\int e\,dt \qquad (2)$$

if the applied voltage is sinusoidal. When the core flux reaches the saturation value the inductance of the core becomes zero, assuming that the slope of the hysteresis loop, and all applied voltage appears across the load and rectifier resistances. The current suddenly increases at saturation from a very small value before saturation. The load, or gate, current for a half cycle of operation is shown in Figure 8. For a full-wave type rectifier this wave-shape is repeated each half-

---

[1] Ramey, R. A., On the Control of Magnetic Amplifiers, Trans. AIEE, Vol. 70, Part II, pp. 2124-2128.

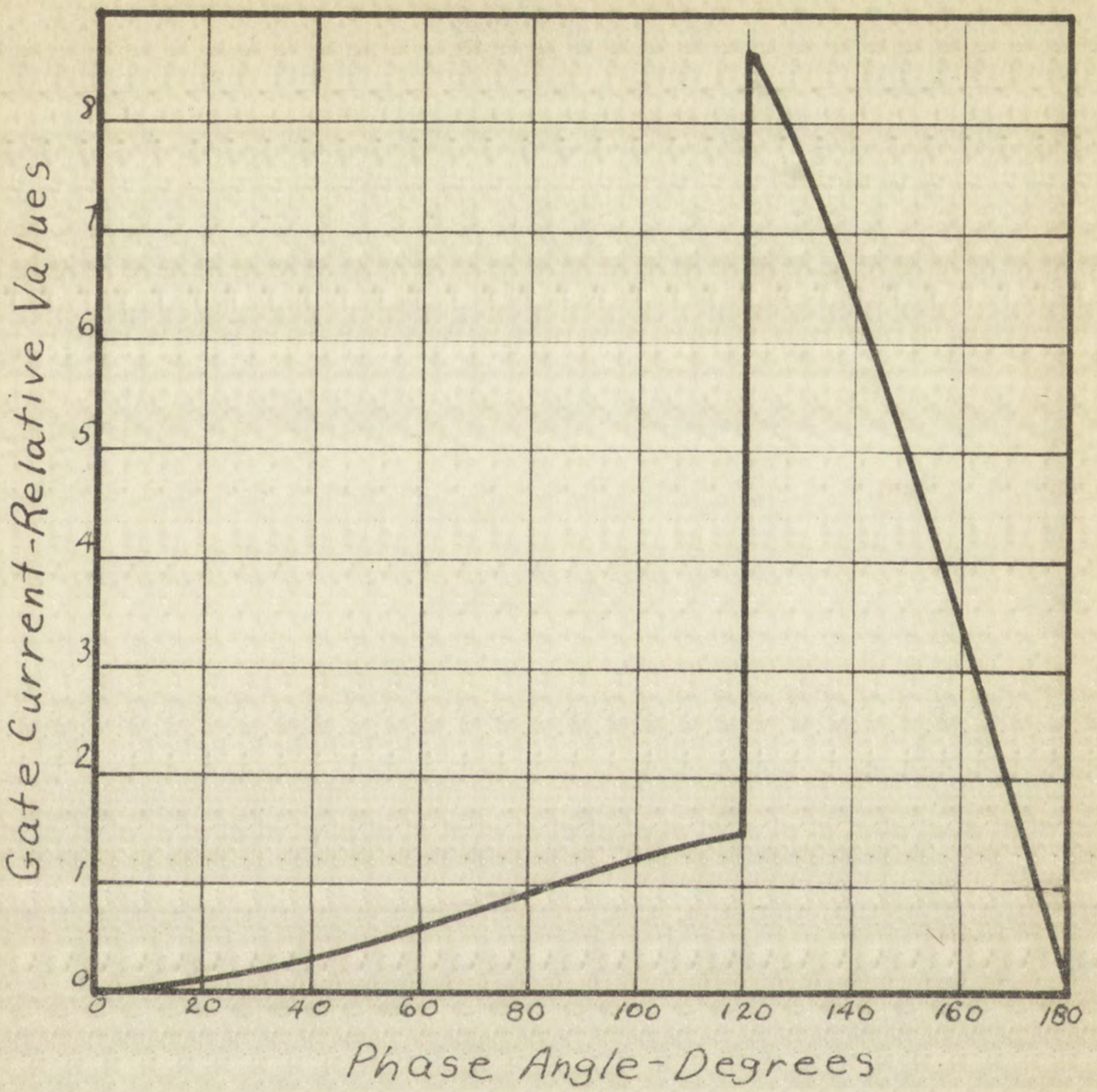

Figure 8

Gate Current of a Magnetic Amplifier

cycle, the two gate windings conducting alternately.

The approximate direct-current load voltage may be found by calculating the direct-current voltage available due to the conducting period of the amplifier and then multiplying by the ratio of the load resistance to the sum of the load and gate resistances. The gate resistance must include both the winding and rectifier resistances. The equation is

$$E_L = \frac{R_L}{R_L + R_g} \quad \frac{E_m}{\pi} \int_{\phi_f}^{\pi} \sin \phi \, d\phi \qquad (3)$$

or

$$E_L = \frac{R_L}{R_L + R_g} \quad \frac{E_m}{\pi} \left(1 + \cos \phi_f \right) \qquad (4)$$

where R_L is the load resistance, R_g is the gate resistance, E_m is the maximum applied voltage, and ϕ_f is the angle at which the gate winding saturates or "fires", using the terminology of gas tubes.

If the control signal is held constant, the curve for the corresponding load voltage as a function of load resistance is then easily calculated by substitution of various values of load resistance. These curves for constant control signal are straight lines.

If the control voltage, e_c, is changed, then, in general, the flux level of the core at the beginning of a cycle is changed due to the change in control current.

cycle, the two gate windings are conducting alternately.

The output of a direct-current load winding may be found by calculating the time-integral of the voltage pulses due to the conducting windings of the amplifier and then multiplying by the ratio of the load resistance to the sum of the load and gate resistances. The gate resistance must include both the winding and rectifier resistances. The equation is

or

where R_L is the load resistance, R_g is the gate resistance, E_m is the maximum applied voltage, and α is the angle at which the gate windings saturate or "fire," using the terminology of the AIEE.

If the control signal is a direct current, the curve for the corresponding load voltage as a function of load resistance is [illegible] of various values of load resistance. These curves for constant control signal are straight lines.

If the control voltage, e_c, is constant, then, in general, the flux level of the core at the beginning of a cycle is unchanged due to no change in control current.

Saturation is then reached at a different time so that the firing angle is also changed. This in turn changes the output voltage.

As the first step in determining the control characteristics, the current in the gate winding during the non-firing part of the cycle was computed. Under these conditions the supply voltage is applied to a circuit consisting of the gate inductance, L, the gate resistance, R_g, and the load resistance, R_L, in series. The loop voltage equation is

$$E_m \sin \omega t = L \frac{di_{L1}}{dt} + (R_g + R_L) i_{L1} \qquad (5)$$

where ω is the angular frequency of the supply voltage, and i_{L1} is the current in the gate winding and the load during the non-firing part of the conducting half cycle.

Using Laplace transform methods[7], noting that at

$$t = 0 \qquad i_{L1} = 0 \qquad (6)$$

and substituting the equality

$$R = R_g + R_L \qquad (7)$$

---

[7] Gardner, M. F. and Barnes, J. L., Transients in Linear Systems (New York: John Wiley and Sons, Inc., 1951) Vol. I.

the transformed equation was found as

$$E_m \frac{\omega}{s^2+\omega^2} = (SL+R)\, I_{L1}(s) \qquad (8)$$

or

$$I_{L1}(s) = \frac{\omega E m/L}{(S+R/L)(s^2+\omega^2)} \qquad (9)$$

$$= \frac{\omega E_m}{L}\left[\frac{A}{S+R/L} + \frac{B}{s+j\omega} + \frac{B^*}{s-j\omega}\right] \qquad (10)$$

where

$$A = \frac{1}{S^2+\omega^2}\Big|_{s=-\frac{R}{L}} = \frac{1}{\left(\frac{R}{L}\right)^2+\omega^2} \qquad (11)$$

$$B = \frac{1}{(S+R/L)(s-j\omega)}\Big|_{s=-j\omega} = \frac{j\frac{R}{L}-\omega}{2\omega\left(\frac{R^2}{L^2}+\omega^2\right)} \qquad (12)$$

Taking the inverse transform,

$$i_{L1} = \frac{\omega E_m}{L} \left\{ \frac{1}{\left(\frac{R}{L}\right)^2 + \omega^2} \quad e^{-\frac{R}{L}t} + 2\,Re\left[\frac{j\frac{R}{L} - \omega}{2\omega\left(\frac{R^2}{L^2} + \omega^2\right)} e^{-j\omega t} \right] \right\} \qquad (13)$$

$$i_{L1} = \frac{E_m}{Z} \left[\sin\ (\omega t - \varphi) + \frac{\omega L}{Z} e^{-\frac{R}{L}t} \right] \qquad (14)$$

where

$$Z = \sqrt{(\omega L)^2 + R^2} \qquad (15)$$

$$\varphi = \tan^{-1} \frac{\omega L}{R} \qquad (16)$$

If the equality $\theta = \omega t$is used, the equation becomes

$$i_{L1} = \frac{E_m}{Z} \left[\sin(\theta - \varphi) + \frac{\omega L}{Z} e^{-\frac{R}{\omega L}\theta} \right] \qquad (17)$$

Since the assumption has been made, for this simplified analysis, that $\omega L >> R$ it follows that $Z \cong \omega L$ and $\varphi = \tan^{-1} \frac{\omega L}{R} \cong \tan^{-1} \infty = \frac{\pi}{2}$. In addition the angle θ is never greater than π. With these substitutions the

equation becomes

$$i_{L_1} = \frac{E_m}{\omega L}\left[\sin\left(\theta - \frac{\pi}{2}\right) + e^{-\frac{R}{\omega L}\theta}\right] \qquad (18)$$

or

$$i_{L_1} = \frac{E_m}{\omega L}\left(\cos\theta + e^{-\frac{R}{\omega L}\theta}\right) \qquad (19)$$

If it is assumed that $\omega L = 10R$ at least, and using the fact that $\theta = \pi/2$ at the most, then the maximum value of $R\theta/\omega L$ is $\pi/20$ or 0.157. The maximum change in the exponential term is 1-0.855 or 0.145. In the same time the cosine term changes from minus one to zero. Thus as a first approximation

$$i_{L_1} = \frac{E_m}{\omega L}\left(1 + \cos\theta\right) \qquad (20)$$

Arbitrarily assuming that the core flux with zero control signal is zero after reset, the flux at saturation is

$$\phi_s = \frac{\mu N_c I_c A}{l} + \frac{\mu N_g I_u A}{l} \qquad (21)$$

where μ is the permeability, A is the area, and l is the length of the core. Or

$$\phi_s = \frac{\mu A N_c i_c}{l} + \frac{\mu A}{l} N_g \frac{E_m}{\omega L}(1+\cos\theta_f) \qquad (22)$$

If the value of $(1+\cos\theta_f)$ from this equation is substituted in equation (4) the result is

$$E_L = \frac{R_L}{R_L+R_g} \frac{\omega L l}{A\pi\mu N_g}\left(\phi_s - \frac{\mu A}{l} N_c i_c\right) \qquad (23)$$

Differentiating,

$$\frac{dE_L}{dl_c} = \frac{R_L}{R_L R_g} \frac{\omega L}{\pi} \frac{N_c}{N_g} \qquad (24)$$

This may be put in a slightly different form by substituting

$$\omega = 2\pi f \quad , \quad L = N_g^2 \frac{\mu A}{l}. \qquad (25)$$

The result is

$$\frac{dE_L}{di_c} = \frac{R_L}{R_L + R_g} \quad \frac{2f\mu A}{l} \quad N_g N_c \tag{26}$$

or

$$\frac{dE_L}{de_c} = \frac{R_L}{R_L + R_g} \quad \frac{2f\mu A}{R_c l} \quad N_g N_c \tag{27}$$

where R_c is the resistance of the control winding.

The point of interest to this discussion is that, if the permeability is constant, then the output voltage is a linear function of control current or voltage. The characteristic curves should then be a set of equally-spaced, parallel lines, ceasing abruptly at the extremes of control, where the core is always saturated or never saturated.

If the core dimensions and permeability, as well as winding data were available, then the static characteristics could be directly computed. Such data were not available for the magnetic amplifier studied. However, oscillograms were available, taken for $e_c = 0$ and $e_c = -52.5$ mV. with a load resistance of 200 ohms. These are shown in Figures 9a and 9b, respectively. From these the corre-

sponding firing angles were found so that a correlation obtained between control current and output voltage. Since practical results showed that for the approximate the control was linear, the family of characteristic curves can be linearly interpolated and extrapolated, and drawn with a slope of $1/2g$. The results of this approximate method are shown in Figure 18.

Since a hysteresis curve of this core was not available it was impossible to predict where control ceased.

The method of calculating the equivalent effective resistance, both for the firing and non-firing conditions is given in Appendix II.

II. THE ACCURACY OF [illegible] METHOD

As the first step in refining the previous approximate analysis, allowance was made for the fact that the current flowing during the non-firing part of each cycle is not exactly a sine function of the time, but is the sum of a cosine and exponential term. For the case of a load resistance of 250 ohms, this current was computed using equation (17). The computed data are presented in Table XII and graphed in Figure 19.

Using the values of firing angle obtained from oscillograms, the value of the gate current at firing was

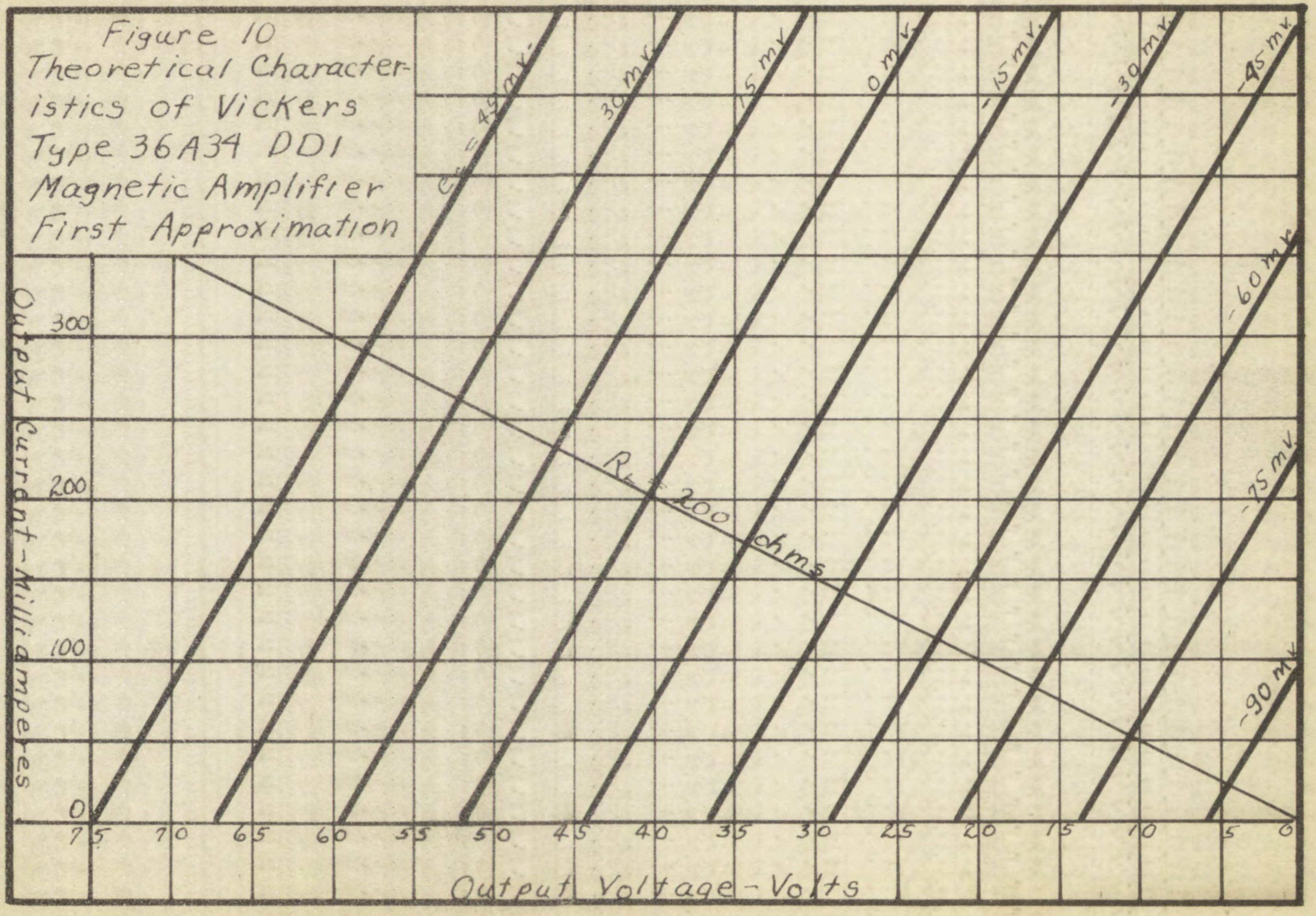

Figure 10
Theoretical Characteristics of Vickers Type 36A34 DDI Magnetic Amplifier First Approximation

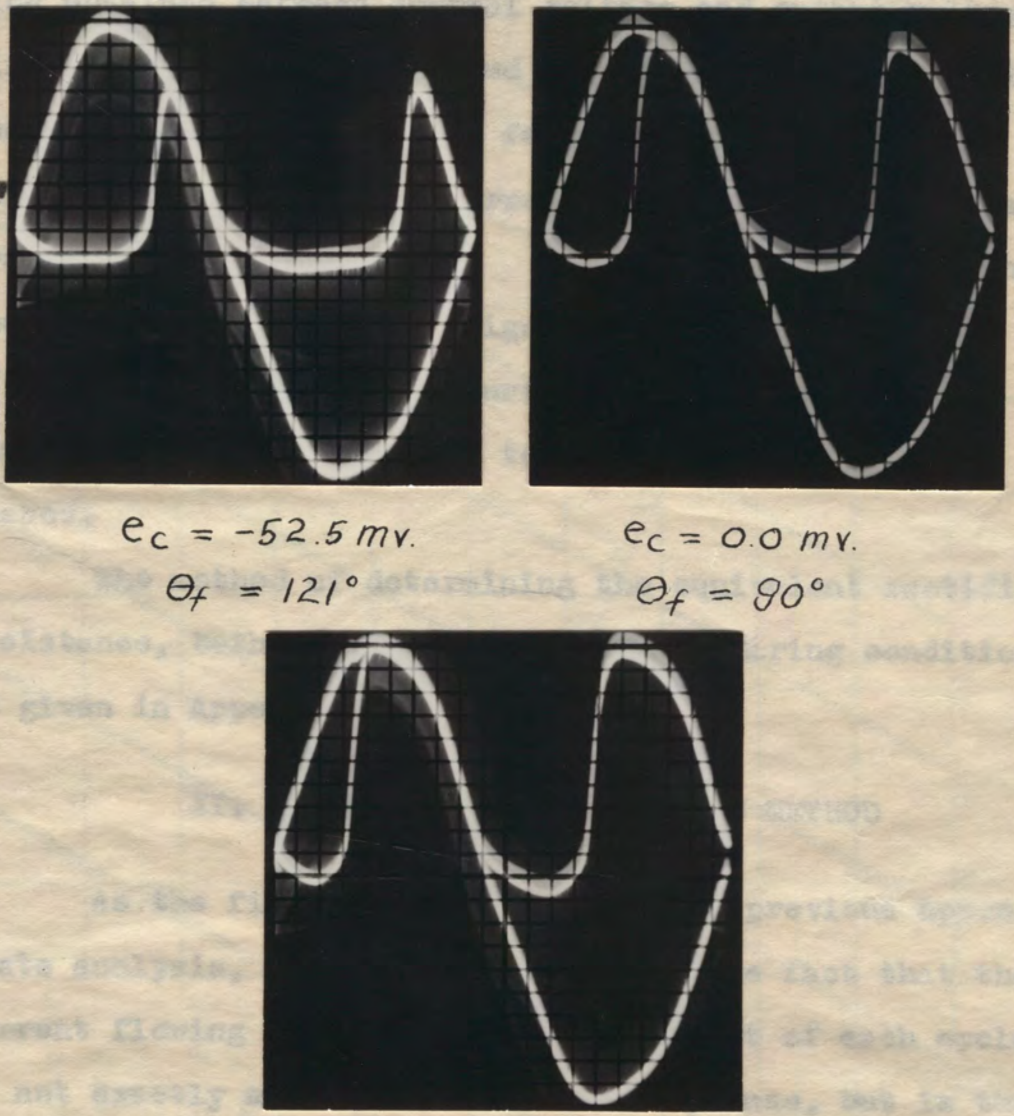

$e_c = -52.5$ mv.
$\theta_f = 121°$

$e_c = 0.0$ mv.
$\theta_f = 90°$

$e_c = +52.5$ mv.

Figure 9

Oscillograms Showing the Variation of Output With Control Signal. $R_L = 200$ ohms

sponding firing angles were estimated and thus a connection obtained between control voltage and output voltage. Since previous results showed that for this approximation the control was linear, the family of characteristic curves can be linearly interpolated and extrapolated, and drawn with a slope of $1/R_g$. The results of this approximate method are shown in Figure 10.

Since a hysteresis curve of the cores was not available it was impossible to predict where control ceased.

The method of determining the equivalent rectifier resistance, both for the firing and non-firing conditions is given in Appendix II.

II. THE REFINED, OR EXTENDED METHOD

As the first step in refining the previous approximate analysis, allowance was made for the fact that the current flowing during the non-firing part of each cycle is not exactly a cosine function in any case, but is the sum of a cosine and exponential term. For the case of a load resistance of 200 ohms, this current was computed using equation (17). The computed data are recorded in Table III and graphed in Figure 11.

Using the values of firing angle determined from oscillograms, the value of the gate current at firing was

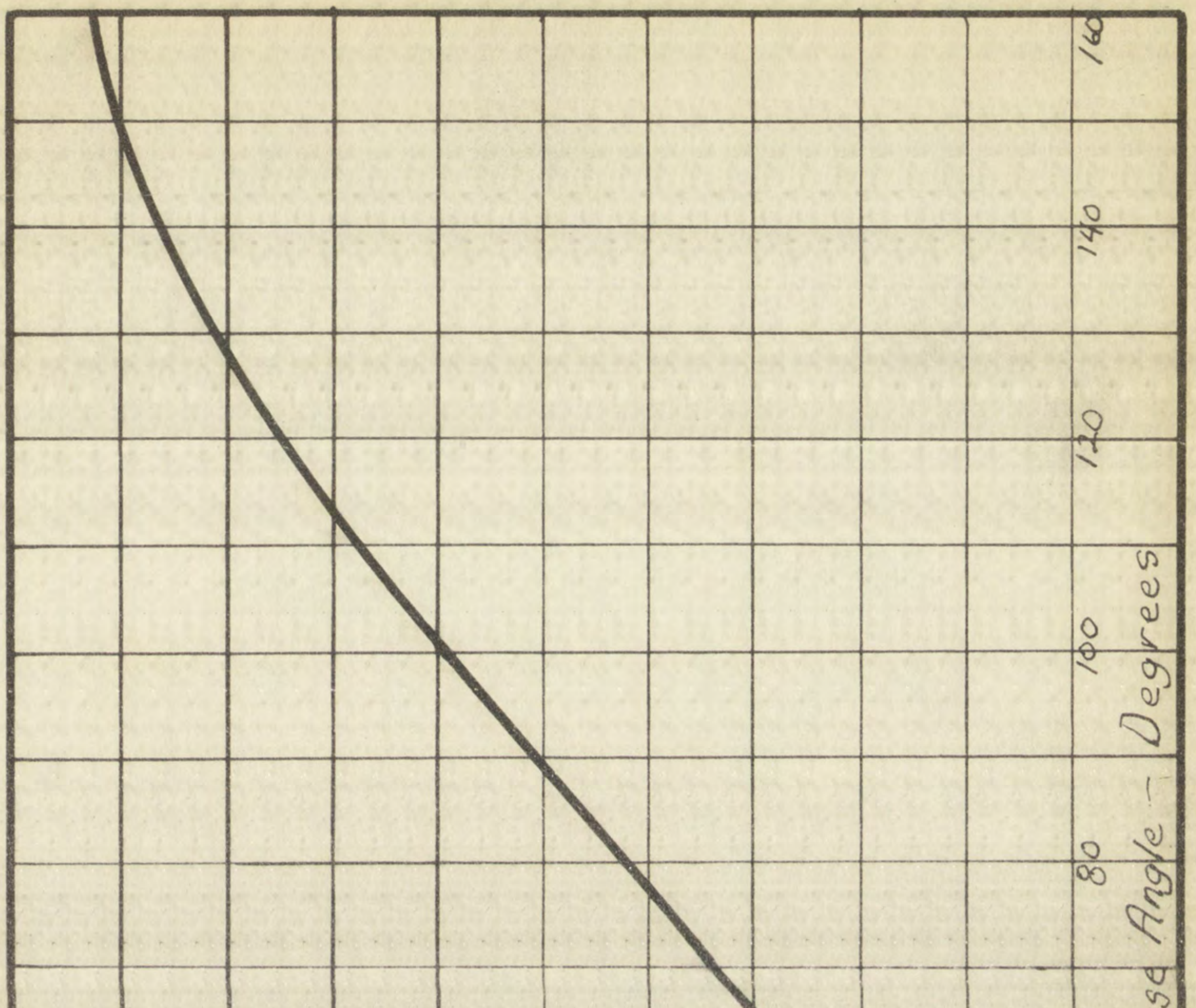

Figure 11
i_{L1} for R_L = 200 ohms
Vickers Magnetic Amplifier
Type 36A39 DDI

determined for the values $e_c = 0$ and $e_c = -52.5$ mv. Using linear interpolation, the firing-time gate current was determined for other values of control voltage. The corresponding values of firing angle were then read from the graph of Figure 11. These values, substituted in equation (4), gave the output for a load of 200 ohms. The new set of characteristic curves was then drawn through this set of points at a slope of $1/R_g$. These curves are shown as the dashed lines in Figure 12.

The next step taken in improving the analysis was to allow for the fact that the current flowing during the non-firing part of the cycle is not zero.

The contribution of the non-firing period to the output voltage is

$$V_1 = \frac{1}{\pi}\int_0^{\theta_f} R_L \, i_{L1} \, d\theta \qquad (28)$$

Substituting the value of i_{L1} from equation (17),

$$V_1 = \frac{E_m R_L}{\pi Z}\int_0^{\theta_f}\left[\sin(\theta-\varphi) + \frac{\omega L}{Z} e^{-\frac{R}{\omega L}\theta}\right] d\theta \qquad (29)$$

determined for the values of [illegible] and [illegible] of Figure [illegible]. Using linear interpolation, the firing-angle curves [illegible] the [illegible] determined for about [illegible] values of [illegible] voltage. The corresponding values of firing angle were [illegible] from the graph of Figure 11. These values, substituted in equation (4), gave the output for a load of [illegible] ohms. The new set of characteristic curves was then drawn through this new set of points at a slope of [illegible]. These curves are shown as the dashed lines in Figure [illegible].

The next step taken to improve the [illegible] was to allow for the fact that the current flowing during the non-firing part of the cycle is not zero.

The contribution of the non-firing current to the output voltage is

[illegible]

Substituting the value of [illegible] from equation [illegible]

[illegible]

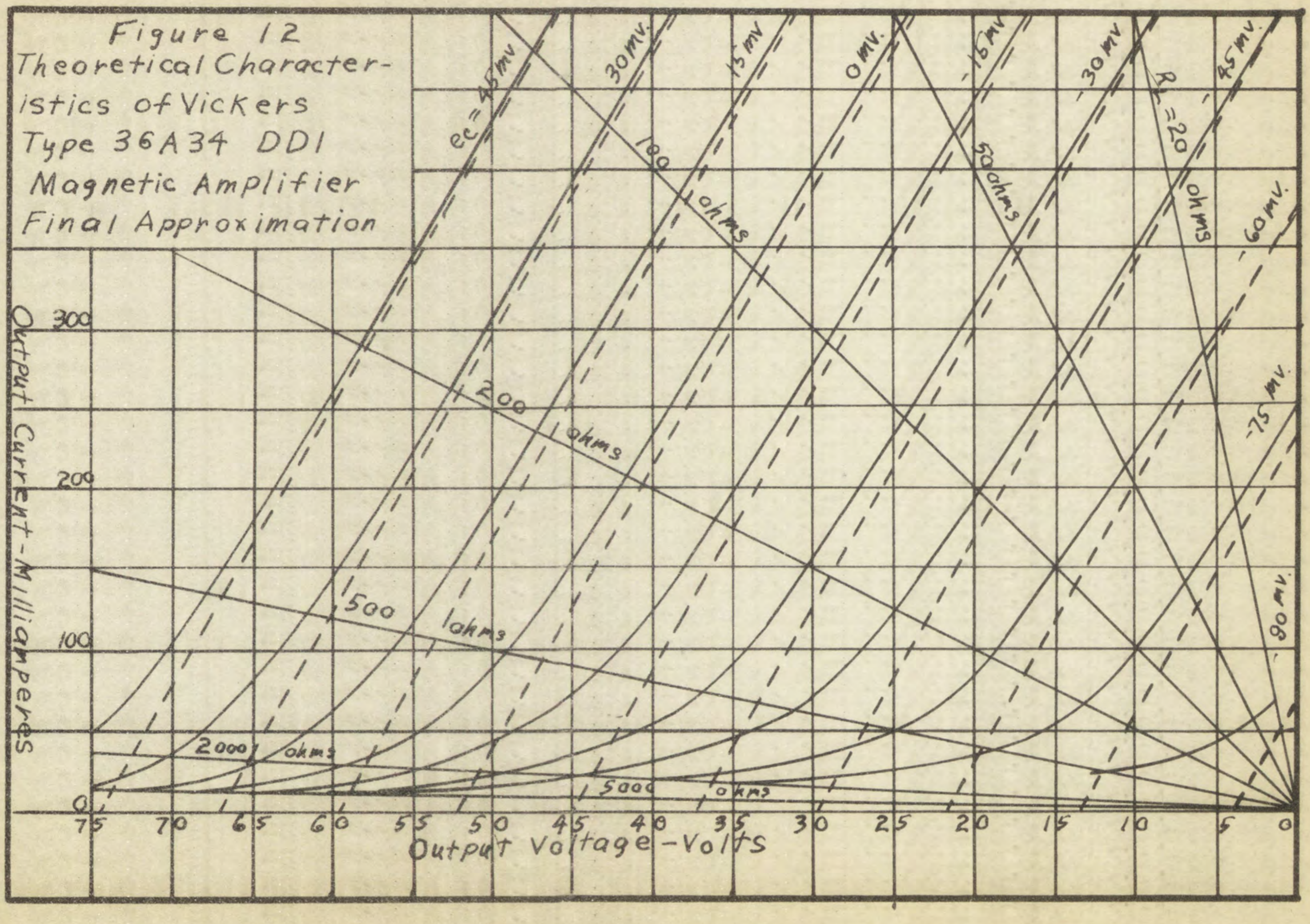

Figure 12
Theoretical Characteristics of Vickers
Type 36A34 DDI
Magnetic Amplifier
Final Approximation

After integrating,

$$V_1 = \frac{E_m R_L}{\pi Z}\left[\cos\varphi - \cos(\theta_f - \varphi) + \frac{\omega^2 L^2}{RZ}\left(1 - e^{-\frac{R}{\omega L}\theta_f}\right)\right] \quad (30)$$

where the angles are in radians.

Using the firing times already computed and several values of load resistance, these data were computed. They have been recorded in Table IV. In Figure 12 these corrections have been added to the results of revision one. The final theoretical characteristic curves are the solid lines.

III. COMPARISON OF THEORETICAL AND EXPERIMENTAL RESULTS

In Figure 13 the final theoretical curves for the magnetic amplifier have been retraced for comparison with the experimental curves. The shape of the final curves is, in general, a much better approximation to the shape of the experimental curves than the first approximation shown in Figure 10.

However, the theoretical calculations are useless for predicting the amplifier characteristics at both extremes of control signal. From the experimental results it is apparent that a control signal of + 30 mv. already

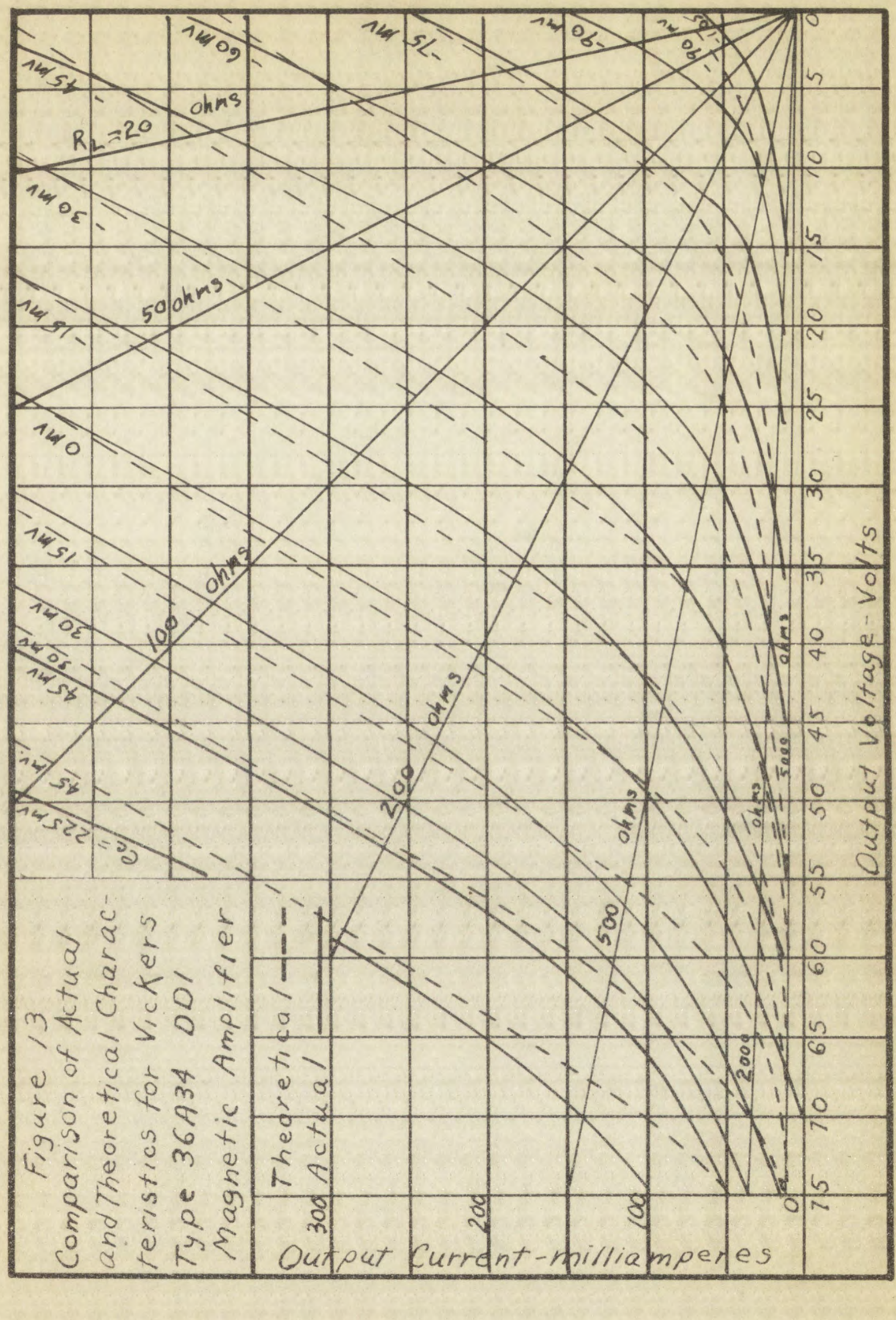

Figure 13 Comparison of Actual and Theoretical Characteristics for Vickers Type 36A34 DD1 Magnetic Amplifier

reaches into the knee of the hysteresis curve and that beyond this point the curve rapidly flattens out so that there is little control. Below -75 mv. control is also poor since the negative control signal is so strong that the peak current flowing after firing drives the flux only into the knee of the hysteresis curve. These two points take account of the fact that although ordinarily a rectangular hysteresis loop is assumed, in practice the loop will always have a rounded transition region. To complete the analysis in these extreme regions it would be necessary to have a hysteresis loop of the core material. Such a curve could not be obtained from the manufacturer, nor was time available to prepare good instrumentation to obtain the hysteresis curve[8].

The theoretical curves would match the experimental ones better if they were shifted slightly to the right. An error of this magnitude might easily have been introduced in determining the firing angle from the oscillograms.

---

[8] Lord, H. W., Dynamic Hysteresis Loop Measuring Equipment AIEE Trans., Vol. 71, Part I, pp. 269-272.

reaches into the knee of the hysteresis curve and that beyond this point [illegible] only partially effective so that there is little control. Under these conditions [illegible] gets poor since the negative control signal is so small [illegible] the peak current [illegible] after firing drives the flux only into the knee of the hysteresis curve. These [illegible] take account of the fact that although ordinarily a rectangular hysteresis loop is assumed, in practice the loop will always have a rounded shoulder region. To complete the analysis in a more rigorous manner it would be necessary to have a hysteresis loop of the core material. Such a curve could not be obtained from the manufacturer, nor was time available to prepare good instrumentation to obtain the hysteresis curve.

The theoretical curves would match the [illegible] ence better if they were shifted slightly to the right. An error of this magnitude might easily have been introduced in determining the firing angle from the oscillograms.

---

[8] [illegible]

CHAPTER IV

SUMMARY, CONCLUSIONS AND RECOMMENDATIONS

I. SUMMARY AND CONCLUSIONS

For experimental determination of the characteristics of a magnetic amplifier, the characteristic curve method was used. The flexibility of the method and ease of obtaining an equivalent circuit were indicated.

For theoretical calculation of the characteristics of a magnetic amplifier, the normal simplifying assumptions were made and applied to the calculation of the characteristic curves, or external characteristics. The limitations of this method were indicated.

Corrections were then made to allow for nonlinearity of control due to the voltage drop across the load resistance and for the increased output due to the current flow during the non-firing part of the cycle.

Comparison of theoretical and experimental results showed that the refined method gave an overall better approximation to the shape of the amplifier characteristic curves, especially for large values of load resistance.

II. RECOMMENDATIONS

Quite obviously the investigation is far from complete. Some points to investigate are listed below.

1. Deviation from Linearity at the Extremes of Control. If considerable care and work were exercised to obtain a good dynamic hysteresis loop of the core material, then the separation of the control curves could be determined graphically.

2. Variation of Firing Angle as a Function of Load Resistance. With the approximations used in this analysis, it appears that the firing angle should increase as the load is increased. However, the oscillograms of Figure 14 did not bear this out, showing that the firing angle was constant for moderate load values and then actually decreased with increasing load in some cases. Here, again, the hysteresis loop could be used to give a better approximation, since the actual current at all times could be calculated, rather than assuming that firing takes place instantaneously. A graphical method might be the easiest for the transition region, for the inductance changes constantly over this region.

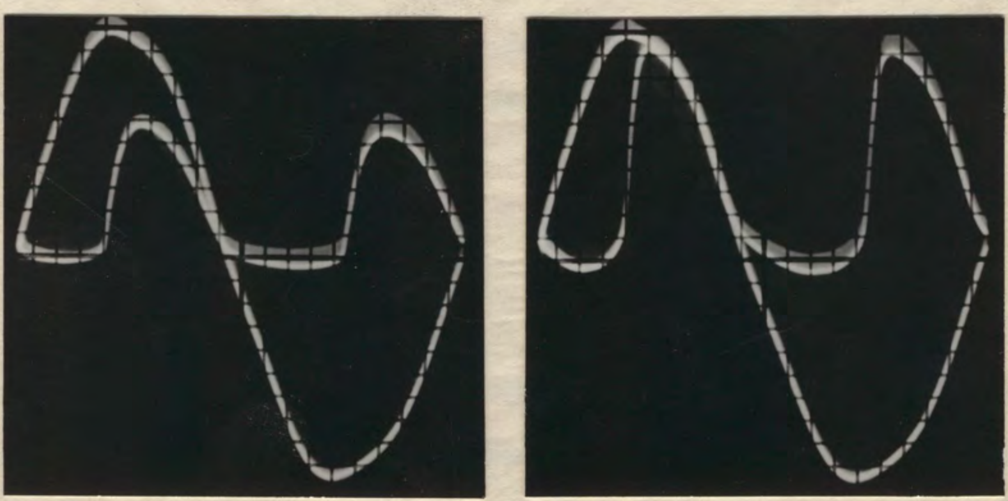

$R_L = 50$ ohms

$R_L = 200$ ohms

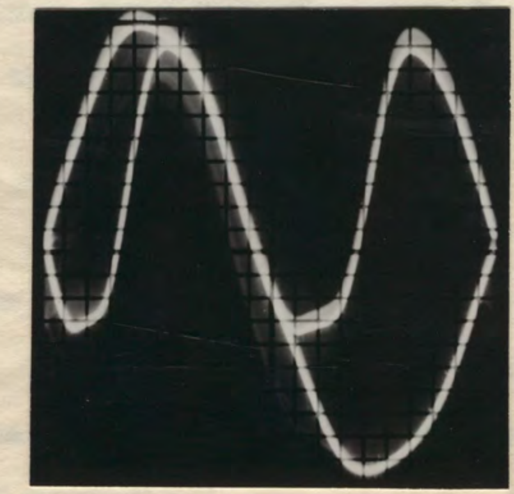

$R_L = 2000$ ohms

Figure 14

Oscillograms Showing the Variation of Output With Load Resistance. $e_c = 0$ mv.

APPENDIX A

COMPUTATION OF EQUIVALENT CIRCUIT PARAMETERS

The value of R_g, the gate or equivalent resistance of the magnetic amplifier was determined from the definition

$$R_g = \left.\frac{\Delta E_L}{\Delta I_L}\right|_{e_c \text{ constant}}$$

Several computations were made over the region from maximum current to a load resistance of 300 ohms. The values were then averaged. The average value obtained for R_g was 58 ohms.

The value of the amplification factor, μ , was determined from the definition

$$\mu = \left.\frac{\Delta E_L}{\Delta e_c}\right|_{I_L \text{ constant}}$$

Several computations over the control region were made and averaged. The average value obtained for μ was 500.

The data for these computations have been recorded in Table VI of Appendix C.

APPENDIX B

DETERMINATION OF EQUIVALENT RESISTANCES OF A RECTIFIER

Since the characteristics of the rectifiers, as shown by Figure 15, are very non-linear, it was necessary to determine linear approximations to these characteristics.

The equivalent resistance of 240 ohms was judged to be a good approximation to the resistance during the non-firing part of a cycle and was used in computations of i_{L1}.

The equivalent resistance of 20 ohms was estimated to be the best fit for currents flowing during the firing part of each cycle and was used to compute the gate resistance, the gate resistance being the sum of winding and rectifier resistances, or 58 ohms.

DETERMINATION OF [illegible]

Since the characteristics of the rectifiers, as shown by Figure 15, were very non-linear, it was necessary to determine linear approximations to these characteristics.

The equivalent resistance of [illegible] ohms was judged to be a good approximation to the resistance during the non-firing part of a cycle and was used in computation of i_{L1}.

The equivalent resistance of [illegible] ohms was estimated to be the best fit for currents flowing during the firing part of each cycle and was used in computing gate resistance, the gate resistance being the sum of winding and rectifier resistances, or [illegible] ohms.

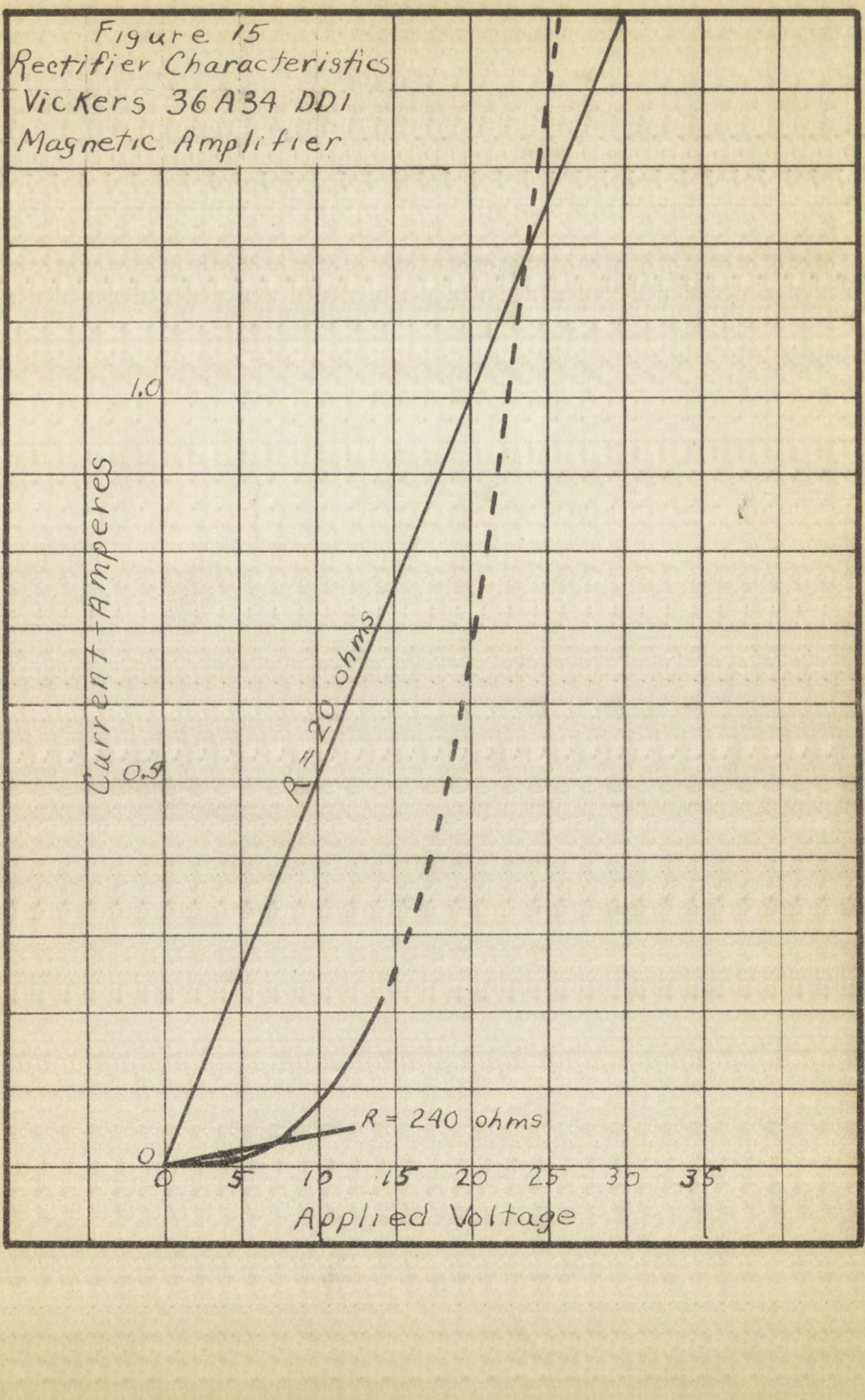

Figure 15
Rectifier Characteristics
Vickers 36A34 DD1
Magnetic Amplifier

APPENDIX C

TABLE I

EXPERIMENTAL DATA FOR THE MAGNETIC AMPLIFIER

Control voltage = +225 mv.		Control voltage = +45 mv.	
E_L	I_L	E_L	I_L
93.0 v.	10.0 ma.	84.5 v.	9.30 ma.
90.0	19.0	80.0	24.5
85.0	37.0	75.0	46.0
80.0	65.5	70.0	72.0
75.0	94.5	65.0	112.
70.0	148.	60.0	163.
65.0	199.	55.5	216.
62.0	245.	52.5	268.
59.0	295.	51.0	316.
56.5	350.	48.6	362.
53.5	402.	44.5	414.
50.0	440.	40.8	474.
49.9	482.		

TABLE I (continued)

EXPERIMENTAL DATA FOR THE MAGNETIC AMPLIFIER

Control voltage = +30 mv.		Control voltage = +15 mv.	
E_L	I_L	E_L	I_L
82.5 v.	8.90 ma.	78.5 v.	8.50 ma.
76.0	28.5	75.0	14.5
70.0	52.5	70.0	31.0
65.0	80.5	66.0	47.0
60.0	125.	61.5	71.0
55.5	169.	57.5	107.
52.0	218.	52.0	160.
50.3	269.	48.6	196.
46.7	323.	45.1	244.
43.3	381.	42.1	291.
38.8	443.	39.1	339.
36.3	489.	36.1	392.
		33.6	444.
		31.2	482.

TABLE I (continued)

EXPERIMENTAL DATA FOR THE MAGNETIC AMPLIFIER

Control voltage = 0 mv.		Control voltage = -15.0 mv.	
E_L	I_L	E_L	I_L
69.0 v.	8.40 ma.	60.0 v.	14.0 ma.
65.0	18.0	55.0	28.0
60.0	34.0	46.9	64.5
55.0	61.5	41.8	106.
50.0	100.	37.2	146.
44.8	151.	33.4	196.
41.2	196.	30.2	243.
37.6	247.	27.5	287.
35.0	293.	26.3	305.
32.2	344.	24.1	344.
29.6	393.	22.6	379.
26.7	449.	19.4	446.
24.8	482.	17.2	489.

TABLE I (continued)

EXPERIMENTAL DATA FOR THE MAGNETIC AMPLIFIER

Control voltage = -30.0 mv.		Control voltage = -45.0 mv.	
E_L	I_L	E_L	I_L
55.0 v.	9.0 ma.	44.4 v.	10.0 ma.
50.0	17.0	42.2	13.0
44.0	35.0	37.2	23.5
39.1	55.5	32.4	36.5
33.2	102.	28.1	57.5
28.8	148.	22.4	105.
24.8	197.	18.5	152.
22.8	232.	16.1	192.
20.0	279.	13.2	247.
19.1	296.	12.4	287.
17.7	322.	10.0	335.
16.0	354.	7.5	389.
15.0	376.	4.3	455.
12.5	432.		
10.8	467.		

TABLE I (continued)

EXPERIMENTAL DATA FOR THE MAGNETIC AMPLIFIER

Control voltage = -60.0 mv.		Control voltage = -75.0 mv.	
E_L	I_L	E_L	I_L
35.8 v.	10.0 ma.	26.4 v.	10.0 ma.
34.4	11.5	21.3	19.0
29.6	19.0	16.5	27.5
24.3	33.5	12.3	49.0
19.1	59.0	7.80	108.
15.3	103.	5.20	146.
12.1	148.	2.55	194.
9.80	196.	0.00	246.
7.20	246.		
5.20	286.		
3.10	329.		
0.00	390.		

TABLE I (continued)

EXPERIMENTAL DATA FOR THE MAGNETIC AMPLIFIER

Control voltage = -90.0 mv.		Control voltage = -105.0 mv.	
E_L	I_L	E_L	I_L
20.5 v.	10.0 ma.	14.8 v.	10.0 ma.
18.2	13.0	11.7	13.5
16.1	15.5	9.80	16.0
12.7	20.0	7.70	19.0
9.80	27.0	5.80	24.0
8.05	33.5	3.75	31.5
4.55	65.5	2.05	44.0
2.50	103.	0.00	66.5
0.00	144.		

TABLE II

CHARACTERISTICS OF THE RECTIFIERS
(VICKERS RECTIFIERS H12CUNICV)

Voltage	Current
0.0 volts	0.000 amperes
2.0	0.000
4.0	0.000
6.0	0.004
8.0	0.033
10.0	0.079
11.8	0.135
13.8	0.196
14.4	0.221

TABLE III

COMPUTED DATA FOR i_{L1}, THE LOAD CURRENT DURING THE NON-FIRING PERIOD

R_L θ	20 ohms i_{L1}	50 ohms i_{L1}
0 deg.	0.0000 amp.	0.0000 amp.
10	0.0004	0.0004
20	0.0016	0.0016
30	0.0035	0.0035
40	0.0061	0.0061
50	0.0092	0.0092
60	0.0129	0.0129
70	0.0169	0.0169
80	0.0211	0.0211
90	0.0255	0.0255
100	0.0299	0.0298
110	0.0341	0.0339
120	0.0379	0.0378
130	0.0413	0.0412
140	0.0442	0.0439
150	0.0464	0.0462
160	0.0480	0.0477

TABLE III (continued)

COMPUTED DATA FOR i_{L1}, THE LOAD CURRENT DURING THE NON-FIRING PERIOD

R_L	100 ohms	200 ohms
Θ	i_{L1}	i_{L1}
0 deg.	0.0000 amp.	0.0000 amp.
10	0.0006	0.0005
20	0.0016	0.0017
30	0.0035	0.0035
40	0.0061	0.0061
50	0.0092	0.0092
60	0.0129	0.0128
70	0.0169	0.0168
80	0.0211	0.0210
90	0.0254	0.0252
100	0.0297	0.0295
110	0.0338	0.0334
120	0.0376	0.0371
130	0.0408	0.0404
140	0.0436	0.0430
150	0.0457	0.0451
160	0.0473	0.0464

TABLE III (continued)

COMPUTED DATA FOR i_{L1}, THE LOAD CURRENT DURING THE NON-FIRING PERIOD

R_L	500 ohms	2000 ohms
θ	i_{L1}	i_{L1}
0 deg.	0.0000 amp.	0.0000 amp.
10	0.0004	0.0003
20	0.0016	0.0015
30	0.0035	0.0033
40	0.0060	0.0057
50	0.0091	0.0085
60	0.0126	0.0116
70	0.0163	0.0149
80	0.0204	0.0182
90	0.0247	0.0215
100	0.0284	0.0246
110	0.0321	0.0273
120	0.0355	0.0297
130	0.0385	0.0314
140	0.0409	0.0326
150	0.0425	0.0331
160	0.0435	0.0329

TABLE III (continued)

COMPUTED DATA FOR i_{L1}, THE LOAD CURRENT DURING THE NON-FIRING PERIOD

R_L	5000 ohms
Θ	i_{L1}
0 deg.	0.0000 amp.
10	0.0004
20	0.0014
30	0.0030
40	0.0051
50	0.0074
60	0.0098
70	0.0123
80	0.0147
90	0.0169
100	0.0188
110	0.0203
120	0.0213
130	0.0218
140	0.0218
150	0.0212
160	0.0201

TABLE IV

V_1, THE CONTRIBUTION OF THE NON-FIRING PERIOD TO THE OUTPUT VOLTAGE FOR VARIOUS LOAD RESISTANCES AND CONTROL VOLTAGES

R_L	20 ohms	R_L	50 ohms
e_c	V_1	e_c	V_1
-30 mv.	0.14 v.	0 mv.	0.23 v.
-45	0.18	-15	0.29
-60	0.22	-30	0.36
-75	0.27	-45	0.45
-90	0.34	-60	0.56
		-75	0.70
		-90	0.94

TABLE IV (continued)

V_1, THE CONTRIBUTION OF THE NON-FIRING PERIOD TO THE OUTPUT VOLTAGE FOR VARIOUS LOAD RESISTANCES AND CONTROL VOLTAGES

R_L	100 ohms	R_L	200 ohms
e_c	V_1	e_c	V_1
45 mv.	0.18 v.	45 mv.	0.38 v.
30	0.26	30	0.50
15	0.35	15	0.75
0	0.46	0	0.94
-15	0.58	-15	1.13
-30	0.73	-30	1.44
-45	0.90	-45	1.75
-60	1.12	-60	2.25
-75	1.40	-75	2.76
-90	1.88	-90	3.76

TABLE IV (continued)

V_1, THE CONTRIBUTION OF THE NON-FIRING PERIOD TO THE OUTPUT VOLTAGE FOR VARIOUS LOAD RESISTANCES AND CONTROL VOLTAGES

R_L	500 ohms	R_L	2000 ohms
e_c	V_1	e_c	V_1
45 mv.	0.89 v.	45 mv.	3.37 v.
30	1.28	30	4.76
15	1.72	15	6.34
0	2.24	0	8.15
-15	2.83	-15	10.20
-30	3.54	-30	12.64
-45	4.35	-45	15.40
-60	5.37	-60	18.85
-75	6.69	-75	23.10
-90	9.03		

TABLE IV (continued)

V_1, THE CONTRIBUTION OF THE NON-FIRING PERIOD TO THE OUTPUT VOLTAGE FOR VARIOUS LOAD RESISTANCES AND CONTROL VOLTAGES

R_L	5000 ohms
e_c	V_1
45 mv.	7.34 v.
30	10.3
15	13.6
0	17.2
-15	21.2
-30	25.8
-45	30.9

TABLE V

MISCELLANEOUS DATA ON THE MAGNETIC AMPLIFIER VICKERS 36A34, DD1 CONNECTED, EDUCATIONAL MAGNETIC AMPLIFIER

Gate coil inductance	16.5 henry
Gate coil resistance	38.0 ohms
Control winding resistance (Winding C)	6.9 ohms
A. C. Supply:	60 cycles, 230/115 volts
Rated load:	0.35 average amperes
Power output:	20 watts (50° C. vise)
Optimum load:	60 ohms
Rectifiers used:	Two Vickers Type H12CUNICV
Control signal:	Three ampere-turns d. c.

TABLE VI (continued)

DATA FOR COMPUTATION OF EQUIVALENT CIRCUIT PARAMETERS

AMPLIFICATION FACTOR DATA

I_L	E_L	e_c	
0.100 amp.	49.0 v.	0.090 v.	545
0.200	45.8	0.090	509
0.300	37.2	0.075	496
0.400	29.6	0.060	494
0.500	28.3	0.060	472
		Average	503

TABLE VI

DATA FOR COMPUTATION OF EQUIVALENT CIRCUIT PARAMETERS

EQUIVALENT RESISTANCE DATA

e_c	E_L	I_L	R_g
15 mv.	42.3 v.	0.70 amp.	60.4
0	40.5	0.70	57.8
-15	40.6	0.70	58.0
-30	40.6	0.70	58.0
-45	38.4	0.70	54.8
-60	27.5	0.50	57.0
-75	28.6	0.45	63.6
		Average	58.5

APPENDIX D

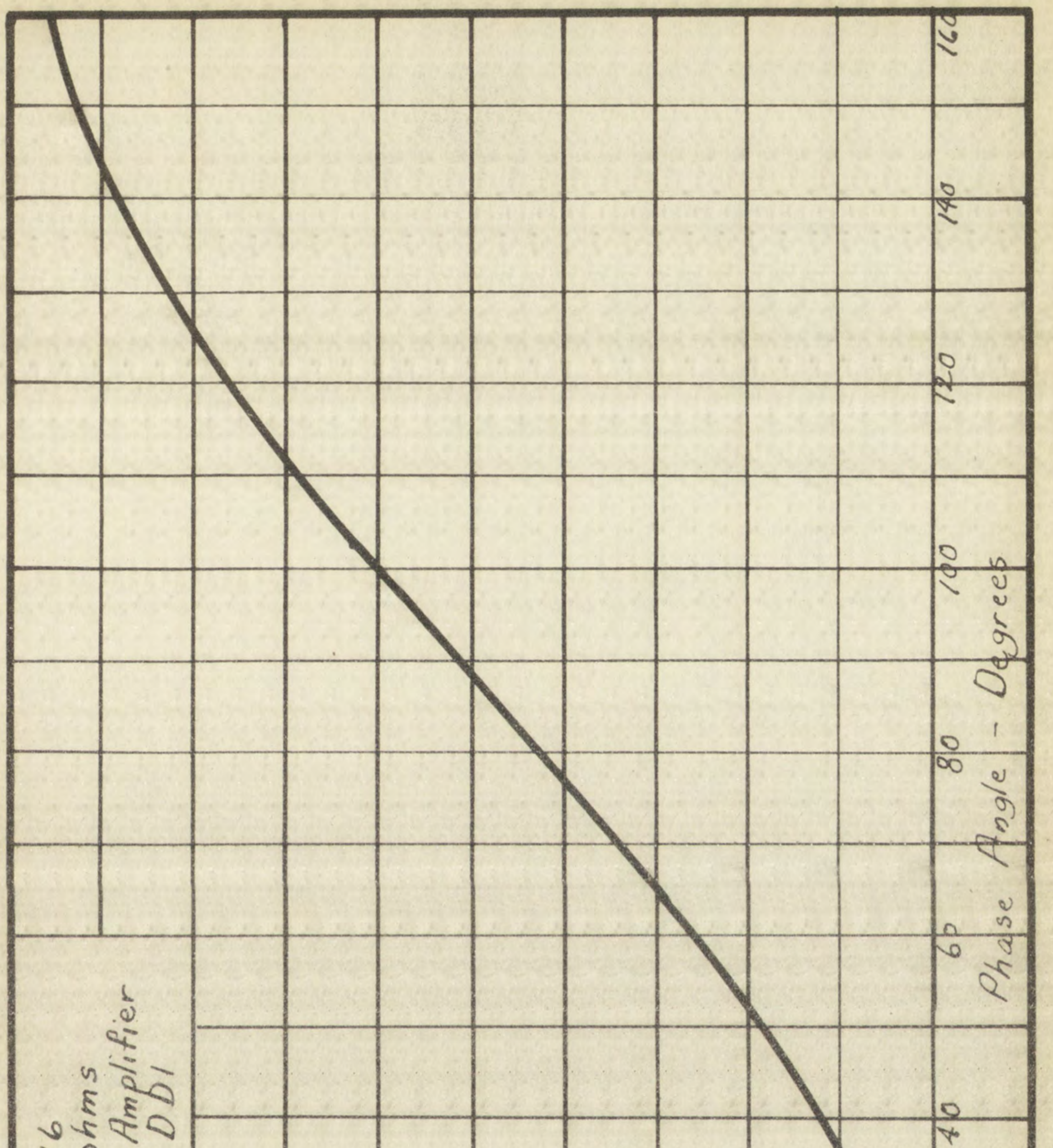

Figure 16

i_L for R_L = 20 ohms

Vickers Magnetic Amplifier

Type 36A34 DD1

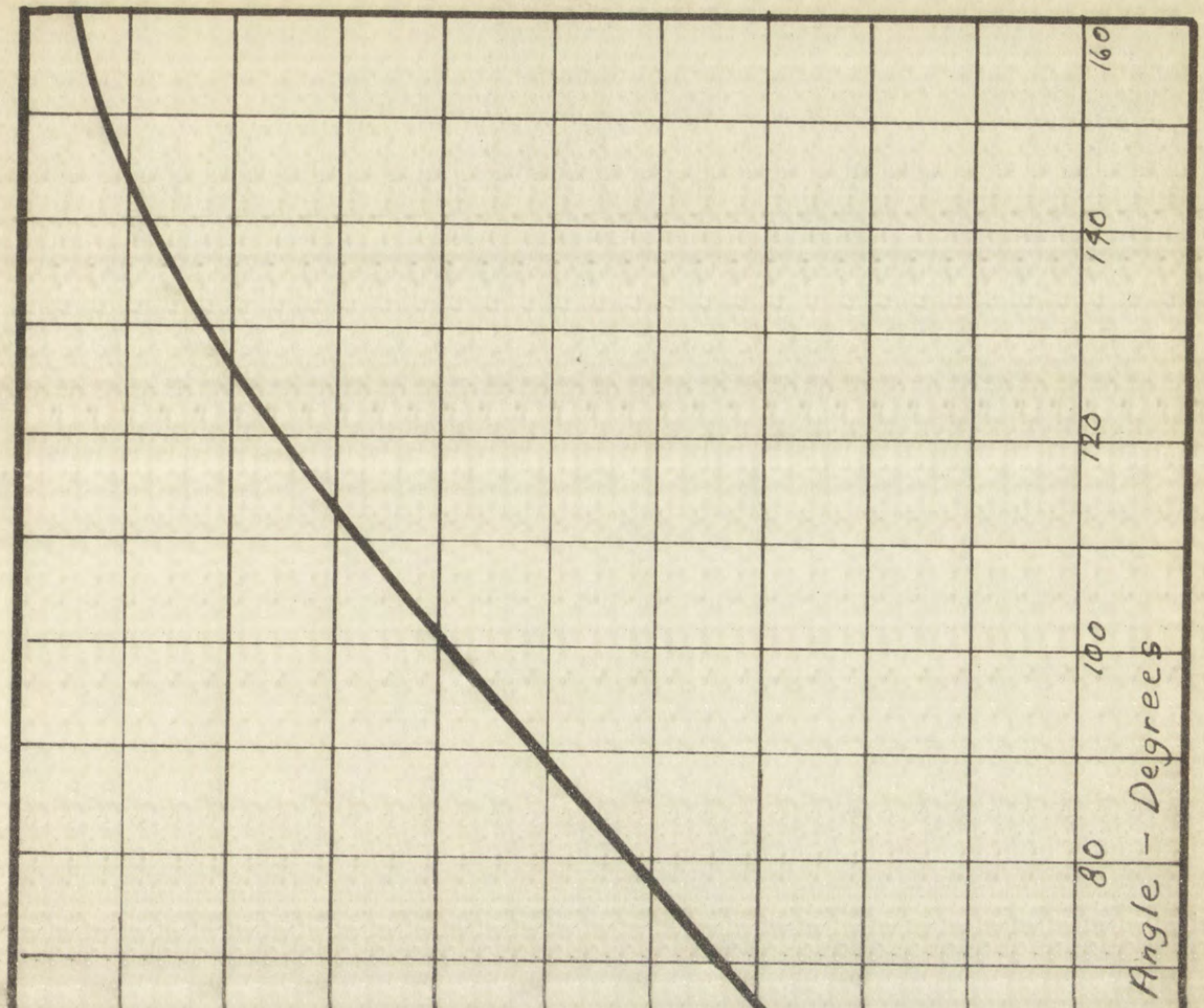

Figure 17

i_{L1} for R_L = 50 ohms

Vickers Magnetic Amplifier

Type 36A34 DDI

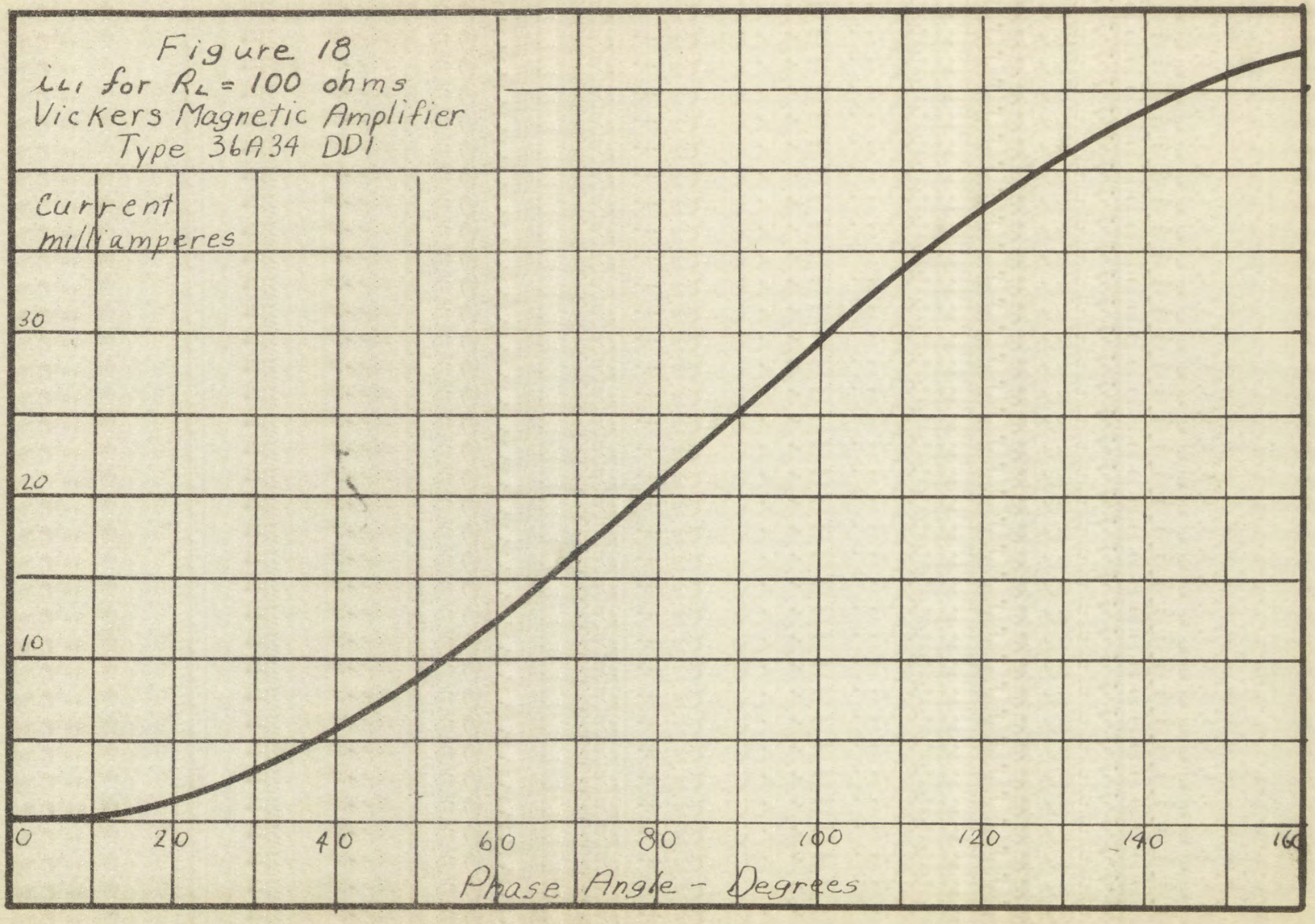

Figure 18
i_{L1} for $R_L = 100$ ohms
Vickers Magnetic Amplifier
Type 36A34 DD1

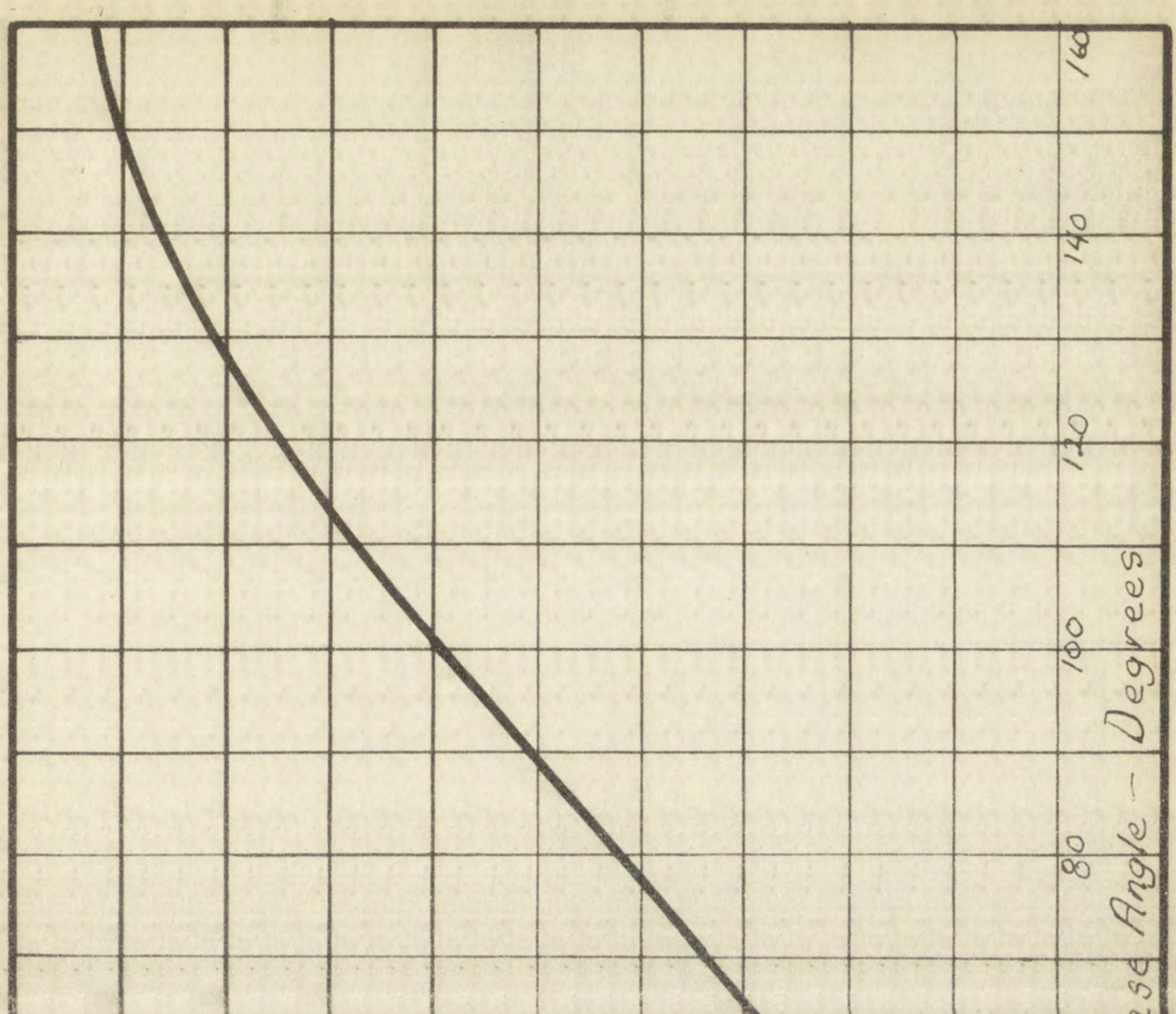

Figure 19
i_{L1} for R_L = 200 ohms
Vickers Magnetic Amplifier
Type 36A34 DDI

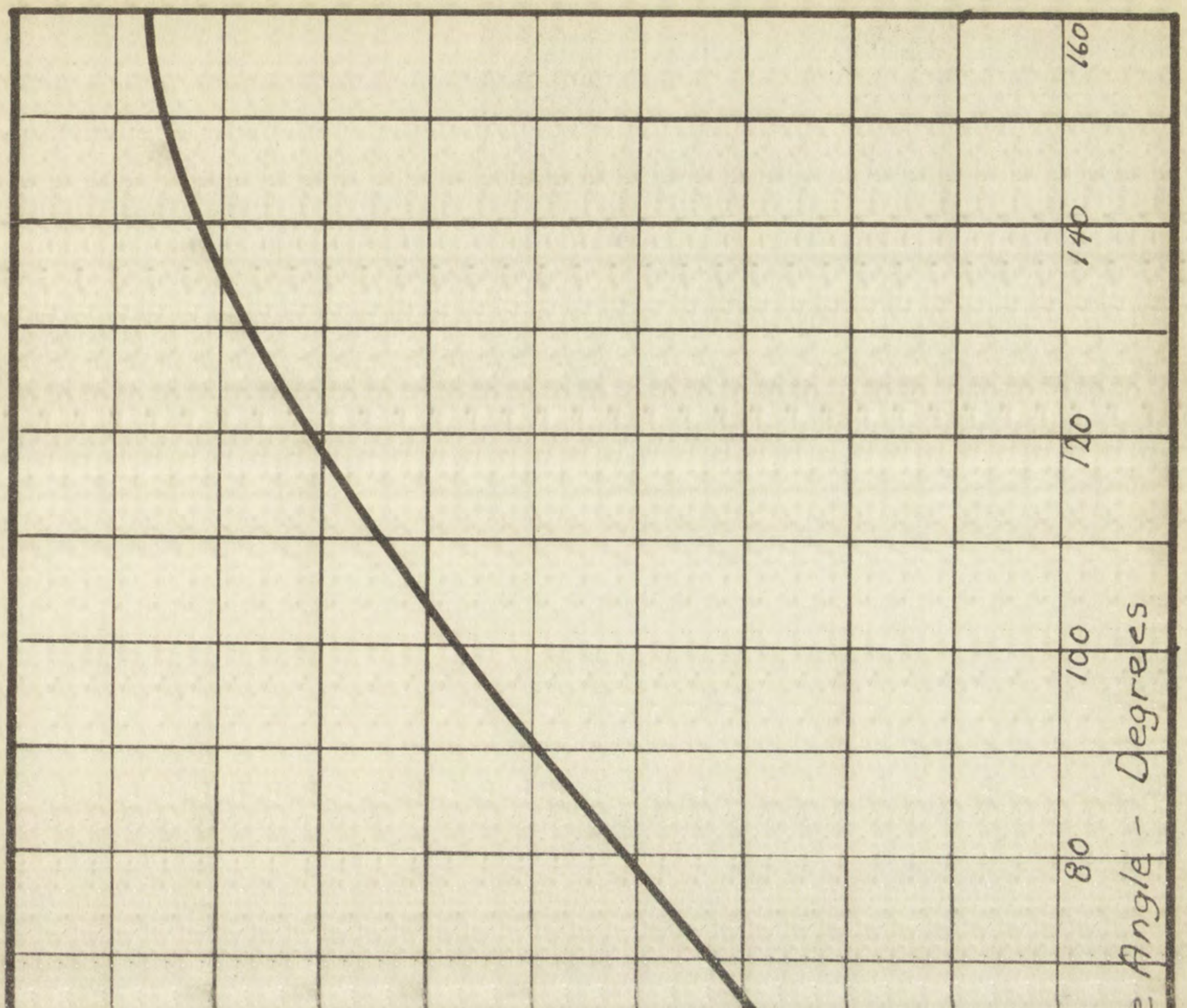

Figure 20
i_{L1} for R_L = 500 ohms
Vickers Magnetic Amplifier
Type 36A34 DD1

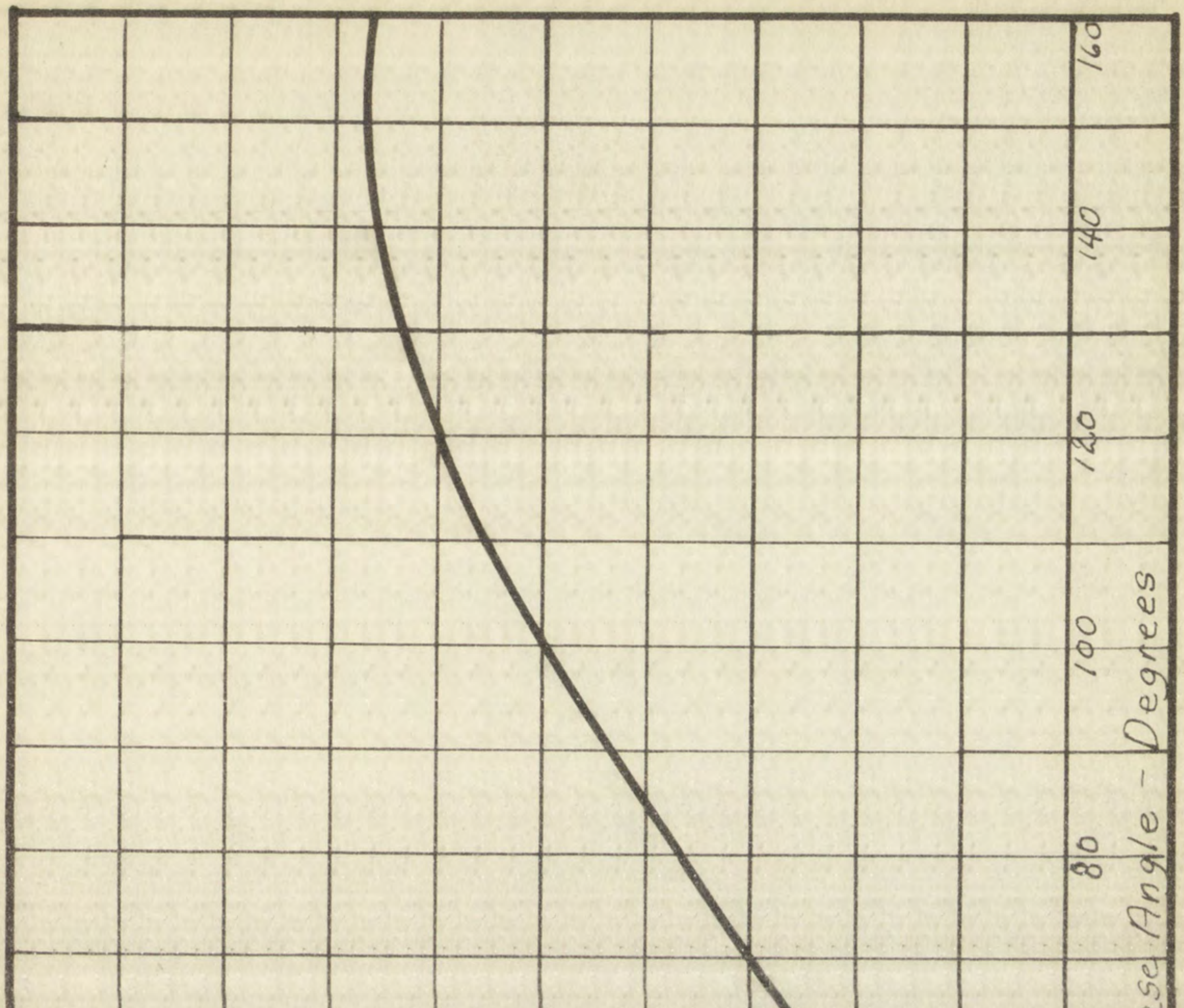

Figure 21
i_{L1} for R_L = 2000 ohms
Vickers Magnetic Amplifier
Type 36 A 34 DD1

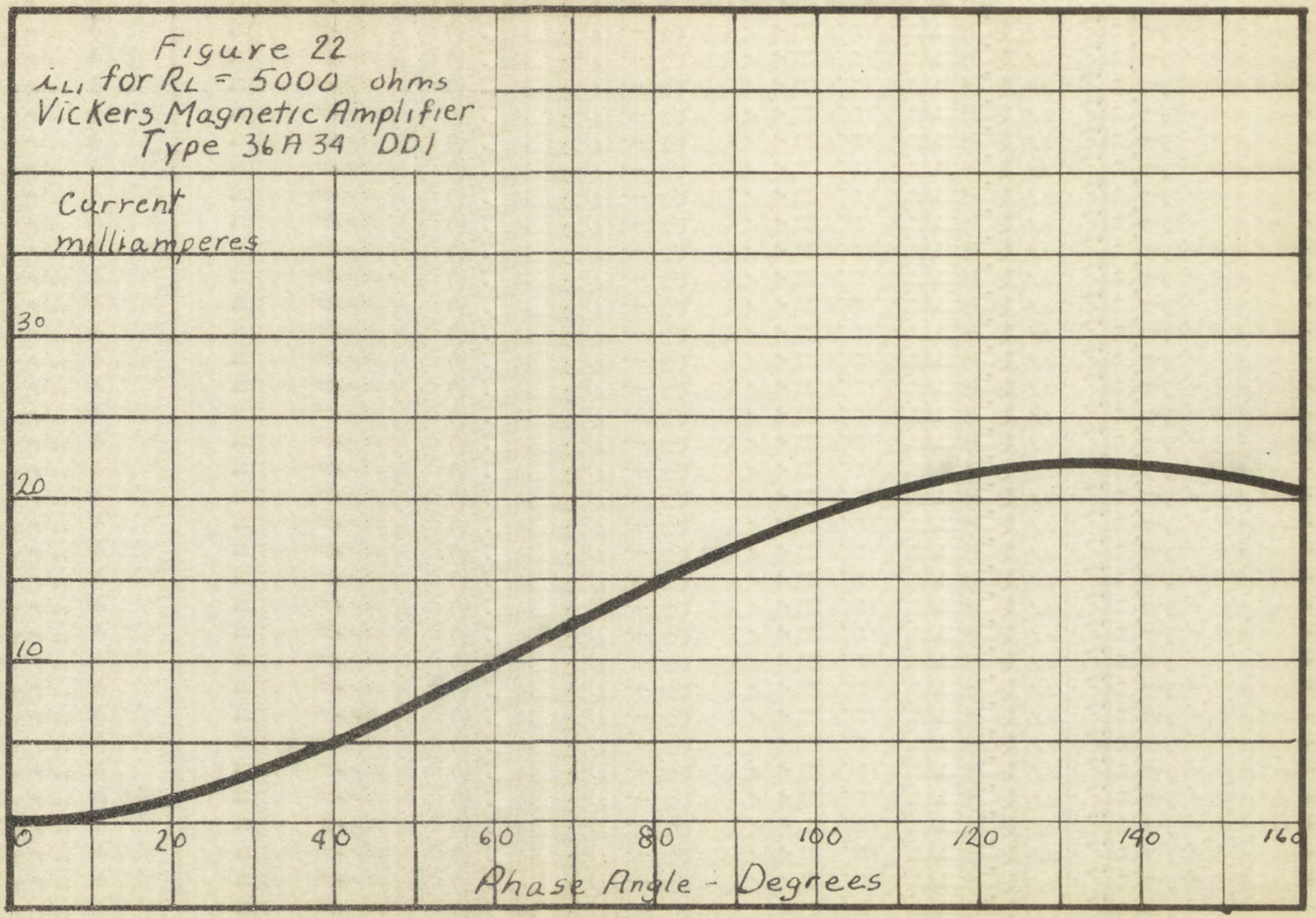

Figure 22
i_{L1} for R_L = 5000 ohms
Vickers Magnetic Amplifier
Type 36A34 DD1

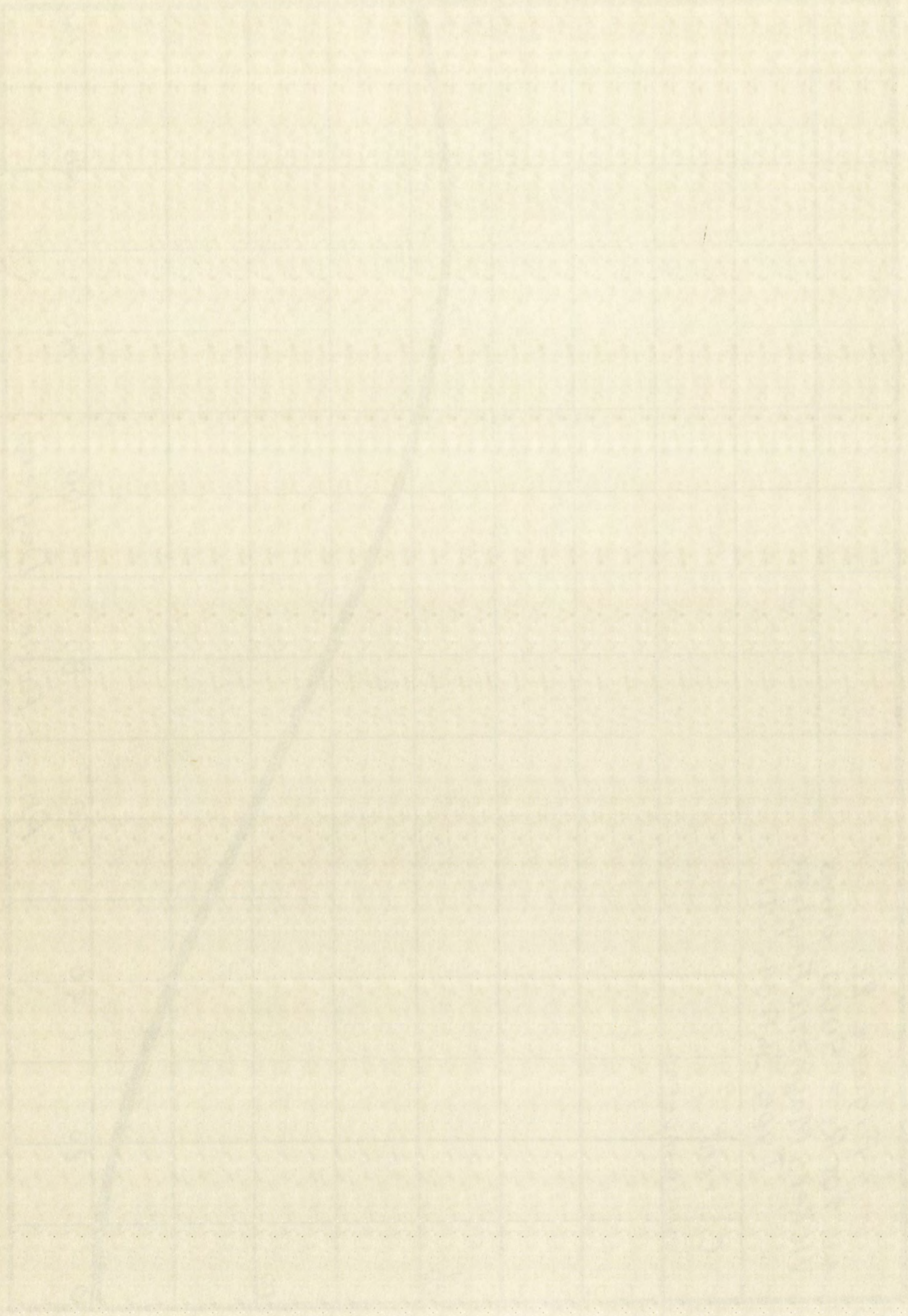

BIBLIOGRAPHY

Davis, W. L. and Weed, H. R., *Industrial Electronic Engineering*. New York: Prentice-Hall, Inc., 1953.

Gardner, M. F. and Barnes, J. L., *Transients in Linear Systems*. New York: John Wiley and Sons, Inc., 1951. Vol. I.

Lord, H. W., Dynamic Hysteresis Loop Measuring Equipment, *Trans*. AIEE., Vol. 71, pp. 269-272.

Martin, Thomas L. Jr., *Electronic Circuits*. New York: Prentice-Hall, Inc., to be published 1954.

Miles, James G., Bibliography of Magnetic Amplifier Devices and the Saturable Reactor Art, *Trans*. AIEE, Vol. 70, pp. 2104-2117.

Ramey, R. A., On the Control of Magnetic Amplifiers, *Trans*. AIEE, Vol. 70, pp. 2124-2128.

Smith, Arthur Whitmore, *Electrical Measurements in Theory and Application*. New York: McGraw-Hill Book Company, Inc., 4th Ed., 1948.

Vickers, *Bulletin 20-B on Magnetic Amplifiers*, Vickers Electric Division, St. Louis, 1950.